Interactome network analysis identifies multiple caspase-6 interactors involved in the pathogenesis of HD.

Riechers, S.P., Butland, S., Deng, Y., Skotte, N., Ehrnhoefer, D.E., Russ, J., Laine, J., Laroche, M., Pouladi, M.A., Wanker, E.E., Hayden, M.R., Graham, R.K.

HMG Advance Access published February 11, 2016

Interactome network analysis identifies multiple caspase-6 interactors involved in the pathogenesis of HD

Sean-Patrick Riechers[1], Stefanie Butland[2], Yu Deng[2], Niels Skotte[2], Dagmar E. Ehrnhoefer[2], Jenny Russ[1], Jean Laine[3], Melissa Laroche[3,4], Mahmoud A. Pouladi[5,6], Erich E. Wanker[1], Michael R. Hayden[2,†] and Rona K. Graham[3,4,*,†]

[1]Max Delbrück Centrum für Molekulare Medizin Berlin-Buch, 13125 Berlin, Germany

[2]Centre for Molecular Medicine and Therapeutics, Child and Family Research Institute, Department of Medical Genetics, University of British Columbia, Vancouver, British Columbia, Canada V5Z 4H4

[3]Department of Pharmacology and Physiology,

[4]Research Center on Aging, University of Sherbrooke, Sherbrooke, Quebec, Canada, J1H 5N4

[5]Translational Laboratory in Genetic Medicine, Agency for Science, Technology and Research

[6]Department of Medicine, National University of Singapore, Singapore 117609

[*]Corresponding Authors: Rona K Graham, PhD, Assistant Professor, Canada Research Chair in Neurodegenerative diseases, Université de Sherbrooke, Faculté de Médecine et des Sciences de la Santé, Département de Pharmacologie et Physiologie, 3001-12ème Avenue N., Sherbrooke, QC, Canada J1H 5N4, T: (819) 346-1110 x 70146, F: (819) 564-5399, E: Rona.Graham@USherbrooke.ca

[†]Co-senior authors

Abstract

Caspase-6 (CASP6) has emerged as an important player in Huntington disease (HD), Alzheimer disease (AD) and cerebral ischemia, where it is activated early in the disease process. CASP6 also plays a key role in axonal degeneration, further underscoring the importance of this protease in neurodegenerative pathways. As a protein's function is modulated by its protein-protein interactions we performed a high throughput yeast-2-hybrid (Y2H) screen against ~17,000 human proteins to gain further insight into the function of CASP6. We identified a high confidence list of 87 potential CASP6 interactors. From this list, 61% are predicted to contain a CASP6 recognition site. Of nine candidate substrates assessed, six are cleaved by CASP6. Proteins that did not contain a predicted CASP6 recognition site were assessed using a LUMIER assay approach and 51% were further validated as interactors by this method. Of note, 54% of the high-confidence interactors identified show alterations in human HD brain at the mRNA level, and there is a significant enrichment for previously validated huntingtin (HTT) interactors. One protein of interest, STK3, a proapoptotic kinase, was validated biochemically to be a CASP6 substrate. Furthermore, our results demonstrate that in striatal cells expressing mutant huntingtin (mHTT) an increase in full length and fragment levels of STK3 are observed. We further show that caspase-3 is not essential for the endogenous cleavage of STK3. Characterization of the interaction network provides important new information regarding key pathways of interactors of CASP6 and highlights potential novel therapeutic targets for HD, AD and cerebral ischemia.

Introduction

Apoptosis, a genetically programmed form of cell death that utilizes caspases, is a fundamental biological process essential for development and regulating the delicate balance between life and death in cells. In neurodegenerative diseases, alterations in components of the cell death machinery occur and enhance apoptosis (reviews (1-3)). Alterations in key components of this death cascade can also have opposite effects and cause uncontrolled cell growth or cancer (reviews (4, 5)). Caspases post-translationally modify their substrates through cleavage at specific recognition sites and cause either inactivation of the protein or a gain of function through generation of active proteolytic fragments. Activation of caspases and proteolytic cleavage of specific caspase substrates is an early, critical cellular event in several neurodegenerative diseases and ischemic brain disorders (6-23). Corroborating their role in neurodegeneration, inhibiting caspases improves neuronal health and behavioral outcomes in models of neurological disease (24-26). Furthermore, environmental enrichment strategies that delay and/or decrease cognitive deficits due to neurological abnormalities are associated with a decrease in caspase expression levels in the brain (27, 28). In contrast, aging, that is characterized by a decline in learning and memory capacity, is accompanied by increased levels of some caspases (15, 17, 29).

Huntington disease (HD), a fatal neurodegenerative disorder characterized by progressive deterioration of cognitive and motor functions, is caused by an expansion of a trinucleotide (CAG) repeat encoding glutamine in the N-terminus of huntingtin (HTT) (30). Neurodegeneration in HD occurs initially and most severely in the medium spiny neurons of the striatum, and later in the deep layers of the cortex (31). In addition to caspase activation, a long-standing hypothesis in neurological disorders such as HD and AD also proposes excitotoxic stress as a key mechanism underlying the pathogenesis of these diseases (6, 8, 10, 32-41). Importantly, HD and AD share a striking number of other similarities including psychiatric symptoms and cognitive dysfunction, increased age-associated risk, neurotrophin depletion and abnormal protein folding

(42). Recently, links between excitotoxic pathways, activation of specific caspases and behavioral deficits have been identified. The evidence suggests that proteolysis of particular caspase substrates may amplify the excitotoxic response and trigger activation of neuronal cell dysfunction, behavioral abnormalities and eventual cell death (6-10, 15, 43). A critical role for excitotoxic stress and caspase activation has also been demonstrated in several models of ischemia (18-20, 22, 23). Indeed, studies of patients, experimental animals and cell culture models in AD, HD and cerebral ischemia provide strong evidence of potential universal mechanisms in the early stages of pathways leading to neuronal death (reviews (1, 2, 42)).

A deeper understanding of caspase substrates and the function of the proteolytic fragments produced upon cleavage is critical for elucidating the mechanism(s) underlying activation of specific apoptotic pathways. Numerous caspase substrates, and the fragments generated post cleavage, have active roles in apoptosis. Indeed, in several experimental paradigms, stress-induced generation of caspase-cleaved proteolytic fragments has been shown to trigger toxicity and amplify the cell death response (44-52). Additional evidence supporting the role of caspase-generated fragments in the pathogenesis of neurodegenerative diseases derives from studies on the caspase resistant form of a caspase substrate. In general, inhibiting the proteolysis of a caspase substrate has been shown to provide protection against cell dysfunction and death (6-8, 14, 15, 43, 49, 51, 53-64).

CASP6 was originally identified as an executioner caspase due to its role in cytoskeletal alterations and cleavage of nuclear lamins. However, CASP6 has since been shown to also function as an initiator caspase through its ability to cleave initiator and executioner caspases (65-67) and activation of CASP6 is observed with aging in the brain and prior to the clinical and pathological diagnosis of both AD and HD (15, 17, 68, 69). Furthermore, preventing CASP6 proteolytic processing of mutant huntingtin (mHTT) or amyloid precursor protein (APP) in HD and AD, respectively, or targeted deletion of CASP6 has been beneficial in these conditions (6-13, 15, 43, 70-72), suggesting that cleavage of other CASP6 substrates may play an

important role in the neurodegeneration observed in these disorders. A role for caspase cleavage (by caspase-7) is also implicated in Spinocerebellar ataxia type 7 (73).

Despite the wealth of evidence demonstrating a central role for CASP6 in neurodegenerative diseases, there has been no systematic study using a high-throughput unbiased approach to identify the CASP6 interactome. To date some CASP6 interactors have been identified, the vast majority are substrates by previous implication in an apoptotic/disease pathway and cleavage site assessment studies (review (1)). There are thus limited details regarding how CASP6 activation leads to neuronal dysfunction and cell death in neurodegenerative diseases. Here we report the first high-throughput study to determine the interacting proteins of the pro and active forms of a caspase. Delineating the global protein-protein interaction (PPI) network of CASP6 and linking proteins with known cellular functions to CASP6 provides important information regarding a key pathway involved in the pathogenesis of neurodegenerative diseases and highlight potential novel therapeutic approaches for HD, AD and ischemia.

Results

Y2H identification of the PPI network for caspase-6

In order to identify CASP6 interactors we performed an automated Y2H screen. Plasmids were engineered to produce fusion proteins containing the LexA DNA binding domain and human CASP6 proform (p34) or active forms (p20 and p10) and then transformed into the MATa Y2H bait strain. Constructed bait strains were then systematically and individually mated with MATα Y2H prey strains carrying GAL4 activation domain fusion constructs of ~17,000 human sequence-validated non-redundant cDNAs from the human ORFeome collection (74, 75). Both the proform and active forms of the CASP6 protein were screened in order to provide additional information about a potential role of the identified substrates and possible

regulators of CASP6. After mating in a matrix assisted approach, protein interactions were identified by yeast growth competence on selective SD4 plates as well as β-galactosidase activity. Potential false positive interactors were excluded from the results based on a list of proteins that show up in high frequency in previous screens with diverse bait proteins. We also excluded interactors that frequently provided a signal with different other bait proteins included in the screening campaign the CASP6 constructs were part of. Based on that a high confidence list of CASP6 interactor proteins was generated which includes 87 proteins that were positive in all three replica of the screen for growth competence under selective conditions *and* in addition were positive at least twice in the LacZ assay (Fig.1A,B, Sup. Table 1). Of the proteins identified as CASP6 interactors, 30 (34%) bind to all three CASP6 baits (p34, p20 and p10). Additionally, 24 (28%) of the proteins interacted with both p20 and p10 active forms of CASP6 (Fig.1C). Assessment of CASBAH and MEROPS databases [of caspase substrates] revealed that none of the identified 87 interactors were previously described CASP6 substrates with the exception of HTT(6, 54) and CASP6 itself (through autoactivation (76)). We also assessed the list in Panther (77) and GO databases to determine if there was any enrichment for specific functions and/or pathways. There was no over-representation after Bonferroni correction for function. However, there was a significant enrichment for proteins involved in the Insulin/IGF pathway-protein kinase B signaling cascade on the list of 87 interactors compared to a genome-wide reference list (p=0.002). Insulin receptors are a subgroup of receptor tyrosine kinases that are involved in modulating cell growth and metabolism.

In order to determine if any of the CASP6 Y2H identified interactors contain possible CASP6 recognition sites we assessed the list through SitePrediction (78), a program that predicts the cleavage site of a protease of which some sites are already known. SitePrediction identified 53/87 interactors with one or more predicted CASP6 cleavage sites with 99.9% specificity (Fig.1C). Furthermore, 16/87 proteins are previously characterized disease-related proteins (OMIM database (79), Sup.Table.1).

Validation of caspase-6 Y2H interactions by LUMIER

Proteins identified in the CASP6 Y2H screen that did not contain a predicted CASP6 recognition site (28/87) were further validated using LUMIER, a luminescence-based, mammalian interaction assay (80) designed for the systematic mapping of dynamic protein-protein interaction networks. Six potential casp6 substrates were also included to provide additional validation of their interaction with casp6. Assessing the protein-protein interactions identified in the Y2H study in the LUMIER assay provides additional confidence that the interaction is high-quality, and, importantly observed in mammalian cells. All clones were tested twice in triplicate, and in both possible orientations of the Renilla and Firefly tags (Renilla bait-Fire-prey/Renilla prey-Fire-bait). We accepted an interaction as positive when it was observed at least in one of the two configurations, and when at least 2 experiments in the two repetitions were positive. The results of this experiment demonstrate that 51% of the interactions were confirmed by LUMIER (Fig.2). A similar success rate was also observed when a positive reference set of binary interactions from the literature was examined with the LUMIER assay (81), supporting our hypothesis that high confidence interactions were identified in our Y2H screens.

HTT interacts with caspase-6

We included several HTT fragment clones in the cDNA prey repertoire in order to determine if an interaction between HTT and CASP6 would be detected. As expected, and detected previously (82, 83), the LUMIER assay demonstrates that CASP6 interacts with fragments of wild type and mHTT (Sup.Fig.1). Both p34 and p20 identified the HTT clone HD507-1230 that contains the IVLD CASP6 recognition site. However, CASP6 also interacts with HTT fragments (HD513) that do not contain the 586aa putative CASP6 recognition site suggesting that alternate binding sites for CASP6 are present in the N-terminal region of HTT as has been suggested by previous data (82). Furthermore, in the presence of the expanded

polyglutamine tract, p34 no longer interacted with the HD513 fragment. CASP6 cleavage assays confirm that CASP6 interacts with HTT and generates an ~60 kDa HTT fragment that is detected with both MAB2166 and BKP1 HTT antibodies (Fig.3A,B) consistent with previous findings (6, 54). It is important to note that even at the lowest concentration of recombinant CASP6 the 586aa HTT fragment is detected. Indeed, in our experimental paradigm, CASP6 cleaved HTT more efficiently than all other substrates assessed. Interestingly, there was a significant enrichment of HTT interactors in the list of potential CASP6 interactors. Fully 9/87 are described HTT interators (hypergeometric statistic = 5.6 x 10-8, Fig.3C).

Identification of dysregulated caspase-6 interators in human HD brain

In order to ascertain whether the identified potential CASP6 interactors may play a role in the pathogenesis of HD we first assessed if expression levels of the genes identified in the screen are altered in human HD post mortem brain tissue (grade 1-4) using previously published HD mRNA profiles generated through microarray analysis (84, 85). Of the 87 high-confidence interactors identified, 54% are either up (36%) or down (18%) regulated at the mRNA level in human HD brain compared to control tissues (Fig.3C, Sup.Table.2). Of note, of the genes dysregulated, 14 are altered in grade 1 post mortem HD brain. We then performed a function enrichment analysis using Panther (77) on the CASP6 interactors showing alterations in expression levels in human HD vs. control brain. A significant over-representation of the following pathways is observed: Insulin/IGF pathway-protein kinase B signaling cascade (p=0.002), p53 pathway feedback loops 2 (p=0.02) and PI3 kinase pathway (p=0.02).

We next determined if any novel and/or previously identified CASP6 interactors showed specific alterations in the caudate nucleus, the region most affected in HD using the INFIDEX method (86). By applying a 3-step expression data filtering strategy (see methods) to all direct interaction partners of CASP6, we identified a caudate nucleus-specific HD network. In the first step, 21 of 121 CASP6 interactors were shown to be

differentially expressed in human brain compared to non-brain tissue and of those, 15 were differentially expressed in the caudate. Lastly, we assessed the 15 caudate specific CASP6 interactors to determine which were dysregulated in HD post mortem tissue compared to controls. Using this step-by-step approach we identified a caudate nucleus-specific HD network comprising 6 dysregulated CASP6 interaction partners namely STK3, VIM, TOP1, PKC, CFLAR, RIMS3 (Sup.Fig.2).

Identification of novel caspase-6 substrates

As CASP6 is activated early in HD, cleavage of other CASP6 substrates in addition to HTT, may contribute to the pathogenesis of HD. Cleavage may result in inactivation of the protein, for example of a pro-survival protein, and reduce the threshold for apoptosis to occur. Cleavage may also result in generation of toxic (pro-apoptotic) fragments, which may then contribute to neuronal dysfunction and/or cell death.

From our list of 87 interactors, 24 (28%) of the proteins were identified with both the p20 and p10 active forms of CASP6. In contrast, only 3 (3%) proteins are in common amongst the p34 proform of CASP6 and p10, and 2 (2%) amongst p34 and p20 baits supporting that some of these proteins may indeed be CASP6 substrates.

Bioinformatic approaches were used as a first step in order to prioritize the identification and characterization of possible CASP6 substrates involved in the pathogenesis of HD (Fig.4). The program SitePrediction (78), predicts that 53/87 CASP6 Y2H identified interactors contain at least one CASP6 cleavage site with 99.9% specificity, 51 of which are expressed in the brain. Subsequent to this, the list was further refined by only including genes implicated in the pathogenesis of HD (alteration in expression levels in human HD brain and/or previously identified HTT interactor) which gave a list of 32 proteins.

In order to increase the likelihood of identifying substrates of CASP6, we chose only those proteins that interacted with both of the active forms of CASP6 (p20 and p10). Finally, in order to identify proteins potentially involved in key signaling pathways in HD, we determined which of the highlighted 21 proteins that bind to both active forms of CASP6 were involved in excitotoxic signaling pathways and/or apoptosis. Filtering the list in a systematic way highlighted the following 9 candidates (Table.1): Brain-specific angiogenesis inhibitor 1-associated protein 2 (BAIAP2), death domain associated protein (DAXX), Glycogen synthase kinase-3 alpha (GSK3A), palmdelphin (PALMD), phosphoinositide-3-kinase, regulatory subunit 1 (alpha) (P13KR1), serine threonine kinase (STK3), RNA binging motif 17 (RBM17), syntaxin 16 (STX16) and ubiquitin specific peptidase (USP32). All candidate proteins are expressed in neurons and due to that a potential neuronal casp6 processing of these candidates might be disease relevant (Sup.Fig.3). This holds true even when the candidate mRNA might be preferentially expressed in another cell type. These proteins were then assessed to determine if they are true CASP6 substrates.

Murine cortex lysates were subject to digestion with increasing concentrations of recombinant CASP6 for one hour or fixed concentration of CASP6 and varying times of incubation. Western blotting demonstrates that CASP6 cleaves DAXX (Fig.5A,B), STK3 (Fig.5C,D), USP32 (Sup.Fig.4A,B), PALMD (Sup.Fig.4C,D), RBM17 (Sup.Fig.5A,B) and STX16 (Sup.Fig.5C,D). Diagrams of each substrate are included which highlight structural domains and potential cleavage sites.

Major CASP6 generated fragments observed for DAXX include 20, 30 and 60 kDa C-terminal fragments. For STK3 we observed two N-terminal fragments of 35 and 45 kDa, for USP32 N-terminal fragments of 80 and 100 kDa, for PALMD 20 and 55 kDa C-terminal fragments, for RBM17 a 60 kDa fragment and for STX16 a 30 kDa fragment. All fragments detected contain the epitope for the antibody used and are of expected sizes based on SitePrediction with the exception of RBM17 and USP32. Cleavage by CASP6 would not generate an 80 kDa USP32 fragment based on SitePrediction predicted (99.9% specificity) cleavage sites.

However it cannot be ruled out that another protease may cleave the CASP6 generated USP32 fragment thus resulting in a smaller sized fragment than expected. With regards to RBM17, no predicted sized fragments were observed. However, we did detect a band at ~70 kDa in size that is cleaved by CASP6. The predicted molecular weight of RBM17 is 45 kDa. However a form of this protein might run higher due to the acidic nature of this protein (pI 5.76) and/or the numerous phosphorylation sites (87). Indeed, 4 separate RBM17 antibodies, which have different epitopes, detect the ~70 kDa band (see Methods).

No cleavage fragments were detected post incubation with recombinant CASP6 for BAIAP2, GSK3A or PIK3R1 (Sup.Fig.6A-C). Overall CASP6 substrate validation of SitePrediction results had a success rate of 67% but in each case SitePrediction did over-predict the number of CASP6 cleavage sites (Table.2). However, this does not exclude the possibility that some fragments may have high turnover rates, that the antibody did not recognize particular fragments and/or the concentration of recombinant CASP6 in our assay was insufficient for certain proteins.

There are now 172 confirmed CASP6 interactors (Sup.Table.3). We included previously published, validated CASP6 interactors (review(1)) and considered preys from the high confidence list that interacted with at least one CASP6 bait in independent assays in both yeast and in mammalian cells as valid interactors. Performing Panther (77) analysis on this list reveals a significant over-representation of several key-signaling pathways post bonferroni correction including FAS signaling, HD, Apoptosis signaling, Gonadotropin releasing hormone receptor and AD-presenilin pathway. There is also a significant enrichment for certain molecular functions including structural constituents of the cytoskeleton, structural molecule activity, protein binding, cysteine-type peptidase activity and peptidase inhibitor activity, and protein classes including cytoskeletal proteins, intermediate filament, structural proteins, actin family cytoskeletal proteins and proteolysis (Table 3).

Alterations in STK3 observed in cellular model HD

We next evaluated whether full length and/or fragment levels of the pro-apoptotic kinase STK3 demonstrate alterations in an acute model of HD. STK3 is a stress-activated pro-apoptotic kinase that upon activation and cleavage enters the nucleus and induces cell death pathways (88-90). We chose to focus on STK3 as alterations in its expression are observed in early grade human HD caudate (84, 85), caspase cleavage is required for activation and toxic fragments are translocated to the nucleus (90) [a key site of pathology in HD], and the fact that STK3 negatively regulates AKT(91) a key protein involved in the pathogenesis of HD (review(92)). Immortalized murine striatal cells with ($STHdh^{Q111}$) and without ($STHdh^{Q7}$) mHTT were serum starved and assessed for protein expression of STK3 using Western blotting (Fig.6A). Activation of CASP6 is observed in this HD model (N. Skotte, personal communication) and is associated with increased cell death (93). A significant increase in full-length levels of STK3 is observed in striatal cells expressing mHTT compared to wild type (WT) at baseline (Fig.6B, ANOVA $p=0.017$, post-hoc $p<0.05$). Importantly, a significant increase in the 35kDa STK3 fragment levels is observed in neurons expressing mHTT compared to WT cells post serum starvation (Fig.6C, ANOVA $p=<0.0001$, post-hoc $p<0.0001$). Evaluation of lactate dehydrogenase (LDH) release (marker of cell death) demonstrates that cell death is observed with serum starvation in this model, consistent with previous findings (93) (Fig.6D, 3 h -serum vs. +serum $p>0.05$; 12 h post starvation, Q111, $p<0.01$).

Cleavage of STK3 in the absence of caspase-3

As caspase cleavage of STK3 has only been previously attributed to caspase-3 (CASP3) in the literature (90), we next wished to determine if cleavage of STK3 occurs in the absence of CASP3. We first show that both recombinant CASP3 and CASP6 generate the same ~35 kDa fragment, while cleavage with CASP6 generates additional 40 and 45 kDa fragments (Fig.7A).

Importantly, we show that cleavage of STK3 is observed in stressed MCF7 cells which do not contain CASP3 (94). Western blotting demonstrates that MCF7 cells stressed with camptothecin show a decrease in full-length STK3 levels and increase of STK3 fragments compared to unstressed MCF7 cells (Fig.7B). These data demonstrate that CASP6 is able to cleave STK3 and that under conditions of stress STK3 cleavage fragments are generated in the absence of CASP3.

Discussion

Substantial evidence supports a central role for CASP6 in neurodegenerative diseases (6-13, 15-17, 29, 47, 48, 82, 95-97). Activation of CASP6 and not other caspases is observed before onset of motor abnormalities in human and murine HD brain and active CASP6 levels inversely correlate with age of onset of HD (15). Human AD brain also shows a significant increase in CASP6 mRNA (95) and active CASP6 (16, 17, 96). Furthermore, in human brain, levels of CASP6-cleaved-tau correlate with global cognitive scores emphasizing the early nature of CASP6 activation in the degenerative process of AD (17). It is crucial to understand the CASP6 network in order to identify victims and other key players in the cell death pathway. We identified 87 potential CASP6 interactors, 54% of which show alterations in mRNA expression in human HD brain, and we validated 6 novel CASP6 substrates. We further show that protein expression levels and cleavage of STK3, a novel CASP6 substrate identified, are altered in striatal cells expressing mHTT.

In order to understand the dynamic nature of a protein and the pathways in which it is operative, it is important to have a more global view of its function in a biological system. Several innovative approaches, including LC-MS/MS and mRNA display, have been used to identify caspase interactors including substates (98-100). However, this is the first time that an Y2H and LUMIER screening approach has been employed using both the proform and the active form of a capase to identify a caspase interactome. In general overlap between Y2H and MS-based screens is low (~2-5%) suggesting method-specific biases exist and support

studies to validate the interaction directly and/or use multiple methods as we have employed here. One explanation for the occurrence of false negatives in Y2H studies is the lack of the interaction domain in the prey since for numerous proteins only a section of the protein can be expressed. However this is not the case for our screen. Furthermore, the high stringent nature of the Y2H assay will mean that transient interactions, and/or proteins with low expression, may escape detection (101, 102). Also of consideration and a potential source of bias, is that some proteins may not fold properly in yeast, may require post translational modifications not found in yeast and/or an inability of interacting protein to enter the nucleus. It is important to note that our studies used human cDNA clones and we also performed the interaction assay in mammalian cells.

Numerous caspase substrates have active roles in apoptosis, in particular as a result of the fragments generated post cleavage. Proteolytic cleavage of specific caspase substrates is an important cellular event in the pathogenesis of several neurodegenerative diseases (6-15, 17, 21). In HD, the CASP6 generated 586aa HTT fragment is observed in affected brain regions and a murine model expressing the 586aa mutant HTT fragment develops neurological abnormalities similar to those observed in HD mouse models (6, 103). CASP6 cleaved APP fragments are observed early in human AD brain (104) and processing of APP at this site generates a small peptide that is a potent inducer of apoptosis (97). In addition to APP, cleavage of several CASP6 substrates have been detected in human AD brain (48, 105, 106). As an example, p97, a valosin containing ubiquitin dependent ATPase, is cleaved by CASP6 in AD brain and the resultant fragment impairs the proteasome and destabilizes endogenous p97 (48). Importantly, CASP6-cleaved-tau (17, 107) and CASP6-cleaved p97 (48) are detected in mild cognitive impaired and AD human brains, suggesting that the activity of CASP6 precedes the clinical and pathological diagnosis of AD. Of interest, CASP6 cleaved tau is observed in AD and HD brain (15, 17). Of note, inhibiting CASP6 cleavage of APP provides some protection *in vivo* against AD-like phenotype (9-13, 108) and eliminating cleavage at the 586aa CASP6 site of mutant HTT (C6R) is sufficient to preserve neuropathological deficits and behavioral disturbances in a murine

model of HD (6-8, 15, 43) making CASP6 a potential target for therapeutic intervention in neurodegenerative diseases. The fact that the proform of CASP6 only interacts with the 513aa wild type htt fragment and not the mhtt fragment suggests that wild type htt may attenuate CASP6 activation but that mhtt is no longer able to perform this function. This notion is in line with the well-established neuroprotective properties of wild type htt. Indeed, while the mechanism(s) underlying the neuroprotective function of htt are poorly defined, a role for htt as a caspase inhibitor has been demonstrated (109, 110). It is interesting to speculate whether the loss of interaction between the proform of casp6 and mutant htt may contribute to the increased CASP6 activation in HD.

To identify CASP6 interactors of high interest and their relationship to the disease state, we assessed our high-confidence list of CASP6 interactors to determine if any show alterations in HD human brain using microarray datasets previously published (84, 85). Interestingly a significant number show alterations in HD human brain. Of the potential interactors showing alterations, we observe an overrepresentation of the Insulin/IGF pathway-protein kinase B signaling cascade, p53 and PI3 kinase pathways. There are a number of proteins in common in these pathways including PDPK1, P13K3R1, PTEN, AKT and p53 all of which are implicated in the pathogenesis of HD (92, 111-116). P53, a direct regulator of CASP6 (117), is a key protein involved in the cellular stress response and the p53 pathway connected by numerous negative and positive feed back loops including Wnt-beta-catenin, IGF-1-AKT, Rb-E2F, p38 MAP kinase, cyclin-cdk, p14/19 ARF pathways and cyclin G-PP2A, and p73 gene products (review (118)). The PI3 kinase pathway is also involved in several key biological processes including survival, metabolism and gene regulation (review(119)).

We identified and validated several novel CASP6 substrates. DAXX has been previously implicated in stroke-mediated cell death and originally identified as a protein that binds to the death domain of the receptor FAS and potentiates FAS-induced apoptosis (120). Cleavage fragments of DAXX are pro-apoptotic and

activate the JNK pathway in an *in vitro* model (121). Multiple functions have been described including a role as a potent transcription repressor that binds to sumoylated transcription factors and as a suppressor of the neuroprotective protein kinase B (AKT) signaling pathway.mActivation of CASP6 and increases in DAXX are observed in a high glucose-induced apoptosis model (122). Cleavage of DAXX would interfere with its interaction with histone 3.3 due to disruption of its histone-binding domain and may lead to alterations in the deposition of histones on DNA and cause chromatin condensation. Proof of principle studies reveal a marked reduction in infarct size and apoptosis in ischemia induced cell death with knockdown and/or expression of a dominant-negative form of DAXX (120, 123). DAXX is also implicated in AD-mediated cell death (120). Of significance, robust increases in DAXX mRNA are observed in human AD brain (124, 125). DAXX destabilizes ASK1 causing release of GRX1 and TRX1, redox proteins that are involved in stabilizing ASK1 and inhibiting the DAXX-ASK1-JNK toxic cell death pathway. Decreased protein expression of TRX1 is observed in human AD cortex and hippocampus, and overexpression of TRX1 in a cellular model of AD protects against Aß toxicity (126). A diagram of DAXX protein showing structural (coiled coil) and nuclear localization signal (NLS) motifs, and predicted CASP6 recognition sites is included as an example (Fig.5B). Strikingly, the predicted CASP6 recognition sites cluster around the structural and signaling motifs.

Validated substrates also include RBM17 and USP32. Cleavage of RBM17, a protein involved in the splicesome complex, may interfere with its function in mRNA splicing thereby altering the regulation of alternative slicing on a global scale. As an example, the U2A-F homology motif, present in RBM17, mediates protein-protein interactions between factors involved in constitutive RNA splicing(127). Through this domain RBM17 regulates alternative splicing of the apoptosis regulatory gene FAS, a key player in PCD pathways. Importantly, splicing of FAS determines whether it encodes a pro-apoptotic or anti-apoptotic form of the FAS protein. RBM17 induces exon skipping of FAS resulting in production of the anti-apoptotic form(127). Significantly, *in vitro* generated fragments of RBM17 cannot bind an AG-containing RNA ligand (127). CASP6 cleavage of RBM17 may provide the mechanism whereby decreased regulation of FAS

through RBM17 causes a shift towards production of the pro-apoptotic from of FAS. USP32 is a ubiquitin protease and Ca^{++} binding protein know to be involved in protein degradation. *In vitro* generated fragments of USP32 have been shown to have alternate subcellular localizations suggesting possible alternate functions of the protein fragments(128).

A number of serine threonine kinases play important roles in programmed cell death pathways and caspase cleavage of STK3 and STK4 is a known mechanism underlying amplification of the apoptotic response (90, 129, 130). Indeed evolutionary conserved caspase sites in STK3 and STK4 hint at important biological roles for the fragments generated. Furthermore, STK3 and STK4 contain NES and NLS sequences (131) suggesting cleavage by caspases may alter the subcellular localization, substrate specificity and/or protein interactions of the fragments compared to the parent protein. CASP3 has been previously been shown to cleave STK3 and STK4, and CASP6 shown to cleave STK4 (90, 129, 130). Of note, particular fragments of STK4 demonstrate distinct catalytic activity and the function of fragments (pro-apoptotic) differ to that of the parent protein (89, 90). Specifically caspase cleavage removes the inhibitory C-terminal domain and the N-terminal fragment is transported to the nucleus. Importantly, in the context of the pathogenesis of HD, IGF-1 inhibits STK3 cleavage and kinase activity via the PI3K/AKT pathway (91). Once STK3 kinase activity is activated via caspase cleavage (cleavage converts STK3 into constitutively active kinase), phosphorylation of c-Jun, H2B, JNK and p38 occurs and STK3 fragments localize to the nucleus prior to DNA fragmentation, suggesting additional nuclear functions of the STK3 fragments in apoptosis. STK3 is only the third kinase shown to interact with CASP6 (132, 133). However, in general caspases are targets of kinases and phosphatases, which facilitate exquisite calibration of caspase activation(134). Conversely, kinases can be targets of caspases, as in the case of RIPK1 and CASP6 (132), leading to inactivation of the kinase and termination of specific signaling pathways.

The evidence demonstrating CASP6 activation and cleavage of HTT and tau in HD mouse models, but not in the caspase-6-resistant HD mice (15) suggests that proteolysis of CASP6 substrates and generation of fragments plays a crucial role in the amplification of CASP6 activity and neuro-toxic signalling in HD. In both HD and AD alterations in AKT (a substrate of CASP6 (135)), including decreased expression and cleavage fragments are observed, suggesting decreased phosphorylation of STK3 may occur (136, 137). Furthermore, a decrease in IGF-1, a potent upstream activator of AKT, has also been reported in a cellular model of HD and may contribute to the downstream alterations in AKT and consequent effects (138). Microarray studies demonstrate that STK3 mRNA is significantly increased in early grade human HD brain (84). We demonstrate here that alterations in STK3 protein expression levels and post-translational modifications are detected in a cellular model of HD and caspase-mediated generation of STK3 fragments observed under conditions of stress in cells expressing mhtt. CASP6 now links STK3 and DAXX with AKT, JNK and histones in the pathogenesis of neurological disorders and highlights an early role for these substrates in neurodegenerative pathways.

In conclusion, we have identified novel members of the CASP6 interactome and demonstrate that a number of these interactors are involved in key signaling pathways observed in neurodegenerative diseases. These data will empower future investigations into the role of caspases in neurodegenerative diseases and their potential as targets for therapeutic intervention.

Material and Methods

Yeast two-hybrid assay

To create a prey-matrix for interaction mating, the MATα yeast strain L40ccα was individually transformed with pACT4-DM-based plasmids encoding prey proteins. The resulting yeast clones were arrayed in 384-well microtiter plates. cDNA fragments encoding the bait protein fragments (CASP6_p10, CASP6_p20,

CASP6_p34) were subcloned into the yeast expression vector pBTM116-D9 and the resulting plasmids were transformed into the MATa yeast strain L40ccua. The activation of the reporter genes *HIS3, URA3,* and lacZ in autocativation tests as a result of the production of bait proteins were tested systematically. All three bait constructs were non-autoactive, and were taken for interaction mating assays with prey proteins (139). Liquid cultures of MATα yeast strains (preys) were replicated in 384-well microtiter plates using a pipetting robot (Tecan, Freedom EVOware®) and then mixed with bait protein producing MATa strains. For interaction mating, yeast mixtures were transferred onto YPD agar plates using a spotting robot (K4, KBiosystems) and incubated for 48 h at 30°C. After mating, clones were automatically picked from agar plates and transferred into 384-well microtiter plates containing SDII (-Leu-Trp) liquid medium and from there they were spotted onto SDII (-Leu-Trp) agar to select for diploid yeasts carrying both – bait and prey vectors. After incubation for 48 h at 30°C, diploid yeast clones were spotted onto SDIV (-Leu-Trp-Ura-His) agar to detect positive PPIs as well as on high density nylon membranes on top of SDIV agar plates for a LacZ assay. In the lacZ assay ß-galactosidase is produced just in growing cells in which bait and prey proteins interact. After incubation for 3 to 4 days at 30°C, grown colonies were fractured with liquid nitrogen and ß-galactosidase activity was detected using the X-Gal substrate. Digital images were taken from agar plates as well as from high density nylon membranes for Visual Grid software (GPC Biotech) assisted result digitalization. The automated Y2H screen was done in 4 repetitions.

LUMIER assay

For LUMIER assays protein A (PA)-Renilla luciferase (RL)-tagged fusion proteins were co-produced with firefly luciferase (FL)-tagged putative interactor proteins in HEK293 cells. After 48 h protein complexes were co-immunoprecipitated from cell extracts with IgG coated magnetic beads (Dynabeads®; Invitrogen); interactions between bait (PA-RL fusions) and prey proteins (FL fusions) were monitored by quantification of firefly luciferase activities (140). Quantification of Renilla luciferase activity was used to confirm that PA-RL-tagged bait proteins are successfully immunoprecipitated from cell extracts. To detect Renilla and firefly

luciferase based luminescence in samples with fusion proteins the Dual-Glo Luciferase Kit (Promega) was used. Bioluminescence was quantified in a luminescence plate reader (TECAN Infinite M1000). For each interaction both PA-RL and FL interactor fusion combinations were tested. Further on, for each protein pair tested (interaction between selected bait and prey proteins) three different parallel co-immunoprecipitation experiments (Co-IPs A-C) were performed in HEK293 cells, in order to assess the specificity of an interaction. To investigate the interaction between the proteins X and Y the protein pairs (A) PA-RL-X/FL-Y, (B) PA-RL/FL-Y and (C) PA-RL-X/FL were individually co-produced in HEK293 cells. The proteins PA-RL (fusions of protein A and Renilla luciferase) and FL (firefly luciferase) in experiments B and C were used as controls to examine background protein binding. The resulting protein complexes in Co-IPs A-C are systematically analyzed by quantification of firefly luciferase activity. R_op and R_ob binding ratios were obtained by dividing the firefly luminescence activity measured in sample A by activities found in samples B and C. These controls work to measure the protein interaction specificity. Low R_op values are an indication for unspecific prey protein interactions, while low R_ob values indicate unspecific bait protein interactions. Based on empirical studies with a set of well-characterized positive and negative interaction pairs (not shown), we defined that R_op and R_ob binding ratios of >1.5 indicate reliable, specific protein-protein interactions.

Prediction of caspase-6 substrates

Interactors were assessed for predicted caspase-6 cleavage sites using the SitePrediction web tool (HTTp://www.dmbr.ugent.be/prx/bioit2-public/SitePrediction/; REF). As SitePrediction requires protein identifiers (IDs) for input, the DAVID gene ID conversion tool (Accessed Jan 6, 2010; REF) was used to convert Entrez Gene IDs or GenBank IDs to Refseq protein IDs. The 87 interactors were mapped to 135 Refseq IDs because each gene may map to one or more protein isoforms. These were submitted to SitePrediction (Accessed Jan 7, 2010) using the ‘caspase-6_Homo_sapiens_4_2’ cleavage model based on known human caspase-6 cleavage sites in the Merops database. Default parameters were used with the

'extended statistics' setting and a threshold of 70. An interactor was considered a putative caspase-6 substrate if at least one cleavage site was predicted with 99.9% specificity.

Identification of HTT-CASP6 shared interactors

To determine which caspase-6 Y2H interactors are known HTT interactors, we compared to HTT interactor publications (141-143).

Genes dysregulated in human HD brain

Direct interaction partners of CASP6 identified by the Y2H screen or known from the literature were identified as potentially perturbed in HD using a 3-step expression data filtering strategy. Gene expression analysis was carried out using the open source R software packages, available as part of the BioConductor project (www.bioconductor.org). The Gene Atlas data set was normalized using MAS5 (Affymetrix Microarray Suite 5). FDR (false discovery rate) values were computed using the local pooled error approach to identify significantly expressed genes (144). For the detection of dysregulated genes, we computed empirical Bayes moderated t-statistics, which corrects gene expression for the collection site, gender and age. For the three filtering steps we used two publicly available gene expression data sets [Gene Atlas (84, 145)]. In the first filtering step 21 of 121 CASP6 interactors were identified as being differentially expressed (adjusted $p<0.00001$) in human brain compared to non-brain tissues (adrenal gland, heart, kidney, liver, lung, lymph node, muscle, prostate, pancreas, placenta, salivary gland, thymus, thyroid, tonsil, testis, trachea, uterus, and uterine corpus) using the Gene Atlas data set (145). As pathogenesis in HD is brain region specific with neurons in the basal ganglia most severely affected (31), we next analyzed the 21 brain-specific CASP6 interactors for being differentially expressed (adjusted $p<0.001$) in the caudate nucleus (CN) compared to the motor cortex (MC), prefrontal cortex (PFC) and the cerebellum (CE) (84). 15 brain-specific interactors of CASP6 were also differentially expressed in the caudate nucleus. Finally, the caudate nucleus-specific CASP6 interactors were filtered for genes differentially expressed in the caudate nucleus of HD

patient brains and healthy individuals. To define differentially expressed genes, expression profiles of brains of 44 HD patients and 36 healthy individuals were analyzed (84, 85). Only genes with $p<0.001$ were accepted as being differentially expressed in HD patients compared to controls. Using this step-by-step approach the caudate nucleus-specific HD network with 6 potentially dysregulated CASP6 interaction partners was predicted.

Caspase-6 cleavage assays

Five samples, each 30 µg of WT murine cortex protein lysates, were incubated with 0 nM, 30 nM, 300 nM, 3 µM or 30 µM of CASP6 (Enzo Life Sciences, USA) at 37°C for 1 hour; another 4 samples (30 µg of WT cortex lysate) were incubated with 15 µM CASP6 at 37°C for 5 min, 15 min, 30 min or 60 min. Samples were then used for western blotting as described below.

Cell culture and LDH assay

The immortalized striatal neuronal cell lines $STHdh^{Q7}$ and $STHdh^{Q111}$ were cultured at 33°C in Dulbecco's modified Eagle's medium (DMEM, Gibco) supplemented with 10% fetal bovine serum, 100X Penicillin/ Streptomycin (Gibco), 2 mM L-glutamine (Gibco), and 0.5 mg/ml active G418. Cells were grown in a humidified atmosphere containing 5% CO_2 and harvested using 0.25% trypsin-EDTA. For serum deprivation experiments, 600,000 cells were seeded on day one, medium was changed to serum free media on day 2 and cells harvested post 24 hours of starvation. MCF-7 cells were cultured in Dulbecco's modified Eagle medium supplemented with 10% fetal calf serum and 2 mM L-Glutamine. Cells were stressed with 5 µM camptothecin for 16 h in the presence or absence of the caspase inhibitor Q-VD-OPh (1 mM) and harvested by scraping.

Protein analysis and Western blotting

Murine cortical tissue lysates for CASP6 cleavage assays were homogenized in 0.303 M sucrose, 20 mM Tris-HCl pH 7.2, 0.5 mM EDTA and 1 mM $MgCl_2$, without protease inhibitors using a glass-teflon IKA-RW 15 homogenizer (Tekmar Company) at maximum speed and cleared by centrifugation for 5 min at 1300 *g*. Lysates were then run on SDS PAGE and probed with one of the following antibodies: DAXX (Santa Cruz: sc-7152) at 1:200, STK3 (Abcam: ab52641) at 1:2000, PI3RK1 (Abcam: ab90578) at 1:920, PALMD (ProteinTech Group: 16531-1-AP) at 1:800, USP32 (Abcam: ab86792) at 1:2000, RBM17 (ProteinTech Group: 13918-1-AP) at 1:1200, GSK-3α/β (Santa Cruz: sc-7291) at 1:500, BAIAP2 (ProteinTech Group: 11087-2-AP) at 1:2000, STX16 (Proteintech) at 1:500, and Actin (Sigma) at 1:1000. Three additional RBM17 antibodies demonstrate an ~70 kDa band on the datasheet (ProteinTech Group: 15374-1-AP, GeneTex GTX120047 and Abcam ab101441). Cell lysates from immortalized striatal cultures were lysed in single detergent phosphatase (SDP) lysis buffer including protease inhibitors (50 mM Tris pH 8.0, 150 mM NaCl, 1% Igepal/NP40, 40 mM B-gp, 10 mM NaF, 1 mM NaVan, 1 mM PMSF, 5 µM zVAD, and 1X Roche Complete). Protein concentration was measured by DC protein assay kit (Bio Rad, USA). Lysates were then separated on 4-12% Bis-Tris gels (Invitrogen). Following transfer membranes were probed with STK3 antibody and beta-tubulin (1:5000; T4026, Sigma Aldrich). Cell pellets from MCF-7 cultures were lysed in 50 mM HEPES pH 7.4, 100 mM NaCl, 1% Igepal, 1 mM EDTA and 10% glycerol with 4.2 µM Pefabloc and 'Complete' protease inhibitor cocktail (Roche) and protein concentrations determined. Following transfer the membrane was probed with anti-STK3 and anti-Actin antibodies. All immunoblots were prepared following standard procedures and used infrared-labeled secondary antibodies (1:5000; Rockland), Immobilon-PVDF-FL membranes and the Li-Cor Odyssey Infrared imaging system (BioSciences). Quantitative analysis of immunoblotting was based on the integrated intensity from Li-Cor Odyssey software (v2.0). To assess serum starvation-induced cell death in the $STHdh^{Q7}$ and $STHdh^{Q111}$, cells were seeded at 10,000 cells/well in a 96-well plate in complete media. After 24 hours, serum starvation was induced by removing the complete media, washing once with PBS, and adding serum-free media. Control (non-serum starved) cells received

fresh complete media. 24 hours later, media was collected, centrifuged at 2,800 rpm for 4 min at 4 C to remove any cell debris, and the supernatant was collected for LDH activity measurements. The LDH assay was performed accordingly to the manufacturers instructions (Roche Cytotoxicity Detection Kit).

Statistical analysis

Except where noted otherwise, statistical analysis was done using one-way and two-way ANOVA (in cases of significant effect of genotype, post-hoc comparisons between genotypes were performed using Bonferroni). P values, SEM, means and standard deviations were calculated using Graphpad Prism version 6.0. Differences between means were considered statistically significant if $p<0.05$.

Acknowledgements

This work was supported by Canada Research Chair funding (RKG, MRH) and by grants from Canadian Institute of Health Research (MRH), and from BMBF (NGFN-Plus; NeuroNet, 01GS08169-73; MooDS, 01GS08150; Mutanom, 01GS08108; GoBio), EU (EuroSpin, Health-F2-2009-241498 and SynSys, HEALTH-F2-2009-242167) and the Helmholtz Association (MSBN, HelMA, HA-215) to EEW. MAP is supported by a Strategic Positioning Fund for Genetic Orphan Diseases from the Agency for Science Technology and Research, and the National University of Singapore. NS is supported by a Canadian Institute of Health Research postdoctoral salary award. MRH, is a Killam University Professor and holds a Canada Research Chair in Human Genetics. RKG holds a Canada Research Chair in Neurodegenerative diseases.

Conflict on interest statement:

The authors confirm there is no conflict of interest.

References

1 Graham, R.K., Ehrnhoefer, D.E. and Hayden, M.R. (2011) Caspase-6 and neurodegeneration. *Trends Neurosci*, **34**, 646-656.

2 Okouchi, M., Ekshyyan, O., Maracine, M. and Aw, T.Y. (2007) Neuronal apoptosis in neurodegeneration. *Antioxid.Redox.Signal.*, **9**, 1059-1096.

3 Friedlander, R.M. (2003) Apoptosis and caspases in neurodegenerative diseases. *N.Engl.J Med.*, **348**, 1365-1375.

4 Elmore, S. (2007) Apoptosis: a review of programmed cell death. *Toxicologic pathology*, **35**, 495-516.

5 Obexer, P. and Ausserlechner, M.J. (2014) X-linked inhibitor of apoptosis protein - a critical death resistance regulator and therapeutic target for personalized cancer therapy. *Frontiers in oncology*, **4**, 197.

6 Graham, R.K., Deng, Y., Slow, E.J., Haigh, B., Bissada, N., Lu, G., Pearson, J., Shehadeh, J., Bertram, L., Murphy, Z. *et al.* (2006) Cleavage at the caspase-6 site is required for neuronal dysfunction and degeneration due to mutant huntingtin. *Cell*, **125**, 1179-1191.

7 Pouladi, M.A., Graham, R.K., Karasinska, J.M., Xie, Y., Santos, R.D., Petersen, A. and Hayden, M.R. (2009) Prevention of depressive behaviour in the YAC128 mouse model of Huntington disease by mutation at residue 586 of huntingtin. *Brain : a journal of neurology*, in press.

8 Milnerwood, A.J., Gladding, C.M., Pouladi, M.A., Kaufman, A.M., Hines, R.M., Boyd, J.D., Ko, R.W., Vasuta, O.C., Graham, R.K., Hayden, M.R. *et al.* (2010) Early increase in extrasynaptic NMDA receptor signaling and expression contributes to phenotype onset in Huntington's disease mice. *Neuron*, **65**, 178-190.

9 Galvan, V., Gorostiza, O.F., Banwait, S., Ataie, M., Logvinova, A.V., Sitaraman, S., Carlson, E., Sagi, S.A., Chevallier, N., Jin, K. *et al.* (2006) Reversal of Alzheimer's-like pathology and behavior in human APP transgenic mice by mutation of Asp664. *Proc.Natl.Acad.Sci.U.S.A*, **103**, 7130-7135.

10 Saganich, M.J., Schroeder, B.E., Galvan, V., Bredesen, D.E., Koo, E.H. and Heinemann, S.F. (2006) Deficits in synaptic transmission and learning in amyloid precursor protein (APP) transgenic mice require C-terminal cleavage of APP. *J Neurosci*, **26**, 13428-13436.

11 Galvan, V., Zhang, J., Gorostiza, O.F., Banwait, S., Huang, W., Ataie, M., Tang, H. and Bredesen, D.E. (2008) Long-term prevention of Alzheimer's disease-like behavioral deficits in PDAPP mice carrying a mutation in Asp664. *Behav.Brain Res.*, **191**, 246-255.

12 Banwait, S., Galvan, V., Zhang, J., Gorostiza, O.F., Ataie, M., Huang, W., Crippen, D., Koo, E.H. and Bredesen, D.E. (2008) C-terminal cleavage of the amyloid-beta protein precursor at Asp664: a switch associated with Alzheimer's disease. *J Alzheimers.Dis.*, **13**, 1-16.

13 Nguyen, T.V., Galvan, V., Huang, W., Banwait, S., Tang, H., Zhang, J. and Bredesen, D.E. (2008) Signal transduction in Alzheimer disease: p21-activated kinase signaling requires C-terminal cleavage of APP at Asp664. *J Neurochem.*, **104**, 1065-1080.

14 Young, J.E., Gouw, L., Propp, S., Sopher, B.L., Taylor, J., Lin, A., Hermel, E., Logvinova, A., Chen, S.F., Chen, S. *et al.* (2007) Proteolytic cleavage of ataxin-7 by caspase-7 modulates cellular toxicity and transcriptional dysregulation. *J Biol.Chem.*, **282**, 30150-30160.

15 Graham, R.K., Deng, Y., Carroll, J., Vaid, K., Cowan, C., Pouladi, M.A., Metzler, M., Bissada, N., Wang, L., Faull, R.L. *et al.* (2010) Cleavage at the 586 amino acid caspase-6 site in mutant huntingtin influences caspase-6 activation in vivo. *J Neurosci*, **30**, 15019-15029.

16 Albrecht, S., Bogdanovic, N., Ghetti, B., Winblad, B. and LeBlanc, A.C. (2009) Caspase-6 activation in familial alzheimer disease brains carrying amyloid precursor protein or presenilin i or presenilin II mutations. *J Neuropathol.Exp.Neurol.*, **68**, 1282-1293.

17 Albrecht, S., Bourdeau, M., Bennett, D., Mufson, E.J., Bhattacharjee, M. and LeBlanc, A.C. (2007) Activation of caspase-6 in aging and mild cognitive impairment. *Am.J Pathol.*, **170**, 1200-1209.

18 Harrison, D.C., Davis, R.P., Bond, B.C., Campbell, C.A., James, M.F., Parsons, A.A. and Philpott, K.L. (2001) Caspase mRNA expression in a rat model of focal cerebral ischemia. *Brain Res.Mol.Brain Res.*, **89**, 133-146.

19 Singh, A.B., Kaushal, V., Megyesi, J.K., Shah, S.V. and Kaushal, G.P. (2002) Cloning and expression of rat caspase-6 and its localization in renal ischemia/reperfusion injury. *Kidney Int.*, **62**, 106-115.

20 Ferrer, I., Lopez, E., Blanco, R., Rivera, R., Krupinski, J. and Marti, E. (2000) Differential c-Fos and caspase expression following kainic acid excitotoxicity. *Acta Neuropathol.*, **99**, 245-256.

21 Mookerjee, S., Papanikolaou, T., Guyenet, S.J., Sampath, V., Lin, A., Vitelli, C., DeGiacomo, F., Sopher, B.L., Chen, S.F., La Spada, A.R. *et al.* (2009) Posttranslational modification of ataxin-7 at lysine 257 prevents autophagy-mediated turnover of an N-terminal caspase-7 cleavage fragment. *J Neurosci*, **29**, 15134-15144.

22 Taghibiglou, C., Martin, H.G., Lai, T.W., Cho, T., Prasad, S., Kojic, L., Lu, J., Liu, Y., Lo, E., Zhang, S. *et al.* (2009) Role of NMDA receptor-dependent activation of SREBP1 in excitotoxic and ischemic neuronal injuries. *Nat Med*, **15**, 1399-1406.

23 Aarts, M., Liu, Y., Liu, L., Besshoh, S., Arundine, M., Gurd, J.W., Wang, Y.T., Salter, M.W. and Tymianski, M. (2002) Treatment of ischemic brain damage by perturbing NMDA receptor- PSD-95 protein interactions. *Science*, **298**, 846-850.

24 Chen, M., Ona, V.O., Li, M., Ferrante, R.J., Fink, K.B., Zhu, S., Bian, J., Guo, L., Farrell, L.A., Hersch, S.M. *et al.* (2000) Minocycline inhibits caspase-1 and caspase-3 expression and delays mortality in a transgenic mouse model of Huntington disease. *Nat.Med.*, **6**, 797-801.

25 Ona, V.O., Li, M., Vonsattel, J.P., Andrews, L.J., Khan, S.Q., Chung, W.M., Frey, A.S., Menon, A.S., Li, X.J., Stieg, P.E. *et al.* (1999) Inhibition of caspase-1 slows disease progression in a mouse model of Huntington's disease. *Nature*, **399**, 263-267.

26 Peng, J., Wu, Z., Wu, Y., Hsu, M., Stevenson, F.F., Boonplueang, R., Roffler-Tarlov, S.K. and Andersen, J.K. (2002) Inhibition of caspases protects cerebellar granule cells of the weaver mouse from apoptosis and improves behavioral phenotype. *J.Biol.Chem*, **277**, 44285-44291.

27 Rampon, C., Jiang, C.H., Dong, H., Tang, Y.P., Lockhart, D.J., Schultz, P.G., Tsien, J.Z. and Hu, Y. (2000) Effects of environmental enrichment on gene expression in the brain. *Proc.Natl.Acad.Sci. U S A*, **97**, 12880-12884.

28 Nakamura, H., Kobayashi, S., Ohashi, Y. and Ando, S. (1999) Age-changes of brain synapses and synaptic plasticity in response to an enriched environment. *J. Neurosci. Res.*, **56**, 307-315.

29 Jiang, C.H., Tsien, J.Z., Schultz, P.G. and Hu, Y. (2001) The effects of aging on gene expression in the hypothalamus and cortex of mice. *Proc.Natl.Acad.Sci.U.S.A*, **98**, 1930-1934.

30 (1993) A novel gene containing a trinucleotide repeat that is expanded and unstable on Huntington's disease chromosomes. The Huntington's Disease Collaborative Research Group. *Cell*, **72**, 971-983.

31 Vonsattel, J.P., Myers, R.H., Stevens, T.J., Ferrante, R.J., Bird, E.D. and Richardson, E.P., Jr. (1985) Neuropathological classification of Huntington's disease. *J.Neuropathol.Exp.Neurol.*, **44**, 559-577.

32 Beal, M.F., Ferrante, R.J., Swartz, K.J. and Kowall, N.W. (1991) Chronic quinolinic acid lesions in rats closely resemble Huntington's disease. *J. Neurosci.*, **11**, 1649-1659.

33 Graveland, G.A., Williams, R.S. and DiFiglia, M. (1985) Evidence for degenerative and regenerative changes in neostriatal spiny neurons in Huntington's disease. *Science*, **227**, 770-773.

34 Landwehrmeyer, G.B., Standaert, D.G., Testa, C.M., Penney, J.B., Jr. and Young, A.B. (1995) NMDA receptor subunit mRNA expression by projection neurons and interneurons in rat striatum. *J Neurosci*, **15**, 5297-5307.

35 Ferrante, R.J., Kowall, N.W. and Richardson, E.P., Jr. (1991) Proliferative and degenerative changes in striatal spiny neurons in Huntington's disease: a combined study using the section-Golgi method and calbindin D28k immunocytochemistry. *J. Neurosci.*, **11**, 3877-3887.

36 McGeer, E.G. and McGeer, P.L. (1976) Duplication of biochemical changes of Huntington's chorea by intrastriatal injections of glutamic and kainic acids. *Nature*, **263**, 517-519.

37 Zeron, M.M., Hansson, O., Chen, N., Wellington, C.L., Leavitt, B.R., Brundin, P., Hayden, M.R. and Raymond, L.A. (2002) Increased sensitivity to N-methyl-D-aspartate receptor-mediated excitotoxicity in a mouse model of Huntington's disease. *Neuron*, **33**, 849-860.

38 Graham, R.K., Slow, E.J., Deng, Y., Bissada, N., Lu, G., Pearson, J., Shehadeh, J., Leavitt, B.R., Raymond, L.A. and Hayden, M.R. (2006) Levels of mutant huntingtin influence the phenotypic severity of Huntington disease in YAC128 mouse models. *Neurobiol.Dis.*, **21**, 444-455.

39 Parameshwaran, K., Dhanasekaran, M. and Suppiramaniam, V. (2008) Amyloid beta peptides and glutamatergic synaptic dysregulation. *Exp. Neurol.*, **210**, 7-13.

40 Hynd, M.R., Scott, H.L. and Dodd, P.R. (2004) Glutamate-mediated excitotoxicity and neurodegeneration in Alzheimer's disease. *Neurochem. Int.*, **45**, 583-595.

41 Okamoto, S., Pouladi, M.A., Talantova, M., Yao, D., Xia, P., Ehrnhoefer, D.E., Zaidi, R., Clemente, A., Kaul, M., Graham, R.K. *et al.* (2009) Balance between synaptic versus extrasynaptic NMDA receptor activity influences inclusions and neurotoxicity of mutant huntingtin. *Nat.Med.*, **15**, 1407-1413.

42 Ehrnhoefer, D.E., Wong, B.K. and Hayden, M.R. (2011) Convergent pathogenic pathways in Alzheimer's and Huntington's diseases: shared targets for drug development. *Nature reviews. Drug discovery*, **10**, 853-867.

43 Metzler, M., Gan, L., Mazarei, G., Graham, R.K., Liu, L., Bissada, N., Lu, G., Leavitt, B.R. and Hayden, M.R. (2010) Phosphorylation of huntingtin at Ser421 in YAC128 neurons is associated with protection of YAC128 neurons from NMDA-mediated excitotoxicity and is modulated by PP1 and PP2A. *J Neurosci*, **30**, 14318-14329.

44 Dix, M.M., Simon, G.M. and Cravatt, B.F. (2008) Global mapping of the topography and magnitude of proteolytic events in apoptosis. *Cell*, **134**, 679-691.

45 Breckenridge, D.G., Stojanovic, M., Marcellus, R.C. and Shore, G.C. (2003) Caspase cleavage product of BAP31 induces mitochondrial fission through endoplasmic reticulum calcium signals, enhancing cytochrome c release to the cytosol. *J. Cell.Biol*, **160**, 1115-1127.

46 Chan, Y.W., Chen, Y. and Poon, R.Y. (2009) Generation of an indestructible cyclin B1 by caspase-6-dependent cleavage during mitotic catastrophe. *Oncogene*, **28**, 170-183.

47 de Calignon, A., Fox, L.M., Pitstick, R., Carlson, G.A., Bacskai, B.J., Spires-Jones, T.L. and Hyman, B.T. Caspase activation precedes and leads to tangles. *Nature*, **464**, 1201-1204.

48 Halawani, D., Tessier, S., Anzellotti, D., Bennett, D.A., Latterich, M. and LeBlanc, A.C. (2010) Identification of Caspase-6-mediated processing of the valosin containing protein (p97) in Alzheimer's disease: a novel link to dysfunction in ubiquitin proteasome system-mediated protein degradation. *J Neurosci.*, **30**, 6132-6142.

49 Levkau, B., Scatena, M., Giachelli, C.M., Ross, R. and Raines, E.W. (1999) Apoptosis overrides survival signals through a caspase-mediated dominant-negative NF-kappa B loop. *Nat.Cell Biol.*, **1**, 227-233.

50 Mazars, A., Fernandez-Vidal, A., Mondesert, O., Lorenzo, C., Prevost, G., Ducommun, B., Payrastre, B., Racaud-Sultan, C. and Manenti, S. (2009) A caspase-dependent cleavage of CDC25A generates an active fragment activating cyclin-dependent kinase 2 during apoptosis. *Cell Death.Differ.*, **16**, 208-218.

51 Tang, G., Yang, J., Minemoto, Y. and Lin, A. (2001) Blocking caspase-3-mediated proteolysis of IKKbeta suppresses TNF-alpha-induced apoptosis. *Mol Cell*, **8**, 1005-1016.

52 Warby, S.C., Doty, C.N., Graham, R.K., Carroll, J.B., Yang, Y.Z., Singaraja, R.R., Overall, C.M. and Hayden, M.R. (2008) Activated caspase-6 and caspase-6-cleaved fragments of huntingtin specifically colocalize in the nucleus. *Hum.Mol.Genet.*, **17**, 2390-2404.

53 Oliver, F.J., de la Rubia, G., Rolli, V., Ruiz-Ruiz, M.C., de Murcia, G. and Murcia, J.M. (1998) Importance of poly(ADP-ribose) polymerase and its cleavage in apoptosis. Lesson from an uncleavable mutant. *J. Biol. Chem.*, **273**, 33533-33539.

54 Wellington, C.L., Singaraja, R., Ellerby, L., Savill, J., Roy, S., Leavitt, B., Cattaneo, E., Hackam, A., Sharp, A., Thornberry, N. *et al.* (2000) Inhibiting caspase cleavage of huntingtin reduces toxicity and aggregate formation in neuronal and nonneuronal cells. *J.Biol.Chem.*, **275**, 19831-19838.

55 Gafni, J., Hermel, E., Young, J.E., Wellington, C.L., Hayden, M.R. and Ellerby, L.M. (2004) Inhibition of calpain cleavage of huntingtin reduces toxicity: accumulation of calpain/caspase fragments in the nucleus. *J.Biol.Chem.*, **279**, 20211-20220.

56 Rao, L., Perez, D. and White, E. (1996) Lamin proteolysis facilitates nuclear events during apoptosis. *J. Cell. Biol.*, **135**, 1441-1455.

57 Charvet, C., Alberti, I., Luciano, F., Jacquel, A., Bernard, A., Auberger, P. and Deckert, M. (2003) Proteolytic regulation of Forkhead transcription factor FOXO3a by caspase-3-like proteases. *Oncogene*, **22**, 4557-4568.

58 Wang, B., Nguyen, M., Breckenridge, D.G., Stojanovic, M., Clemons, P.A., Kuppig, S. and Shore, G.C. (2003) Uncleaved BAP31 in association with A4 protein at the endoplasmic reticulum is an inhibitor of Fas-initiated release of cytochrome c from mitochondria. *J. Biol. Chem.*, **278**, 14461-14468.

59 Lane, J.D., Lucocq, J., Pryde, J., Barr, F.A., Woodman, P.G., Allan, V.J. and Lowe, M. (2002) Caspase-mediated cleavage of the stacking protein GRASP65 is required for Golgi fragmentation during apoptosis. *J. Cell. Biol.*, **156**, 495-509.

60 Walter, J., Schindzielorz, A., Grunberg, J. and Haass, C. (1999) Phosphorylation of presenilin-2 regulates its cleavage by caspases and retards progression of apoptosis. *Proc. Natl. Acad. Sci. U S A*, **96**, 1391-1396.

61 D'Costa, A.M. and Denning, M.F. (2005) A caspase-resistant mutant of PKC-delta protects keratinocytes from UV-induced apoptosis. *Cell death and differentiation*, **12**, 224-232.

62 Nguyen, M., Breckenridge, D.G., Ducret, A. and Shore, G.C. (2000) Caspase-resistant BAP31 inhibits fas-mediated apoptotic membrane fragmentation and release of cytochrome c from mitochondria. *Mol. Cell. Biol.*, **20**, 6731-6740.

63 Latchoumycandane, C., Anantharam, V., Kitazawa, M., Yang, Y., Kanthasamy, A. and Kanthasamy, A.G. (2005) Protein kinase Cdelta is a key downstream mediator of manganese-induced apoptosis in dopaminergic neuronal cells. *J. Pharmacol. Exp. The.r*, **313**, 46-55.

64 Assefa, Z., Bultynck, G., Szlufcik, K., Nadif Kasri, N., Vermassen, E., Goris, J., Missiaen, L., Callewaert, G., Parys, J.B. and De Smedt, H. (2004) Caspase-3-induced truncation of type 1 inositol trisphosphate receptor accelerates apoptotic cell death and induces inositol trisphosphate-independent calcium release during apoptosis. *J. Biol. Chem.*, **279**, 43227-43236.

65 Van de, C.M., Declercq, W., Van, d.b.I., Fiers, W. and Vandenabeele, P. (1999) The proteolytic procaspase activation network: an in vitro analysis. *Cell. Death.Differ.*, **6**, 1117-1124.

66 Slee, E.A., Harte, M.T., Kluck, R.M., Wolf, B.B., Casiano, C.A., Newmeyer, D.D., Wang, H.G., Reed, J.C., Nicholson, D.W., Alnemri, E.S. *et al.* (1999) Ordering the cytochrome c-initiated caspase cascade: hierarchical activation of caspases-2, -3, -6, -7, -8, and -10 in a caspase-9-dependent manner. *J. Cell. Biol.*, **144**, 281-292.

67 Cowling, V. and Downward, J. (2002) Caspase-6 is the direct activator of caspase-8 in the cytochrome c-induced apoptosis pathway: absolute requirement for removal of caspase-6 prodomain. *Cell Death.Differ.*, **9**, 1046-1056.

68 Ramcharitar, J., V, M.A., Albrecht, S., D, A.B. and Leblanc, A.C. (2013) Caspase-6 activity predicts lower episodic memory ability in aged individuals. *Neurobiology of aging*, in press.

69 LeBlanc, A.C., Ramcharitar, J., Afonso, V., Hamel, E., Bennett, D.A., Pakavathkumar, P. and Albrecht, S. (2014) Caspase-6 activity in the CA1 region of the hippocampus induces age-dependent memory impairment. *Cell death and differentiation*, **21**, 696-706.

70 Gafni, J., Papanikolaou, T., Degiacomo, F., Holcomb, J., Chen, S., Menalled, L., Kudwa, A., Fitzpatrick, J., Miller, S., Ramboz, S. *et al.* (2012) Caspase-6 Activity in a BACHD Mouse Modulates Steady-State Levels of Mutant Huntingtin Protein But Is Not Necessary for Production of a 586 Amino Acid Proteolytic Fragment. *J. Neurosci.*, **32**, 7454-7465.

71 Wong, B.K., Ehrnhoefer, D.E., Graham, R.K., Martin, D.D., Ladha, S., Uribe, V., Stanek, L.M., Franciosi, S., Qiu, X., Deng, Y. *et al.* (2015) Partial rescue of some features of Huntington Disease in the genetic absence of caspase-6 in YAC128 mice. *Neurobiol. Dis.*, **76**, 24-36.

72 Aharony, I., Ehrnhoefer, D.E., Shruster, A., Qiu, X., Franciosi, S., Hayden, M.R. and Offen, D. (2015) A Huntingtin-based peptide inhibitor of caspase-6 provides protection from mutant Huntingtin-induced motor and behavioral deficits. *Hum. Mol. Gene.t*, **24**, 2604-2614.

73 Guyenet, S.J., Mookerjee, S.S., Lin, A., Custer, S.K., Chen, S.F., Sopher, B.L., La Spada, A.R. and Ellerby, L.M. (2015) Proteolytic cleavage of ataxin-7 promotes SCA7 retinal degeneration and neurological dysfunction. *Hum. Mol. Genet.*, **24**, 3908-3917.

74 Rual, J.F., Hirozane-Kishikawa, T., Hao, T., Bertin, N., Li, S., Dricot, A., Li, N., Rosenberg, J., Lamesch, P., Vidalain, P.O. *et al.* (2004) Human ORFeome version 1.1: a platform for reverse proteomics. *Genome research*, **14**, 2128-2135.

75 Lamesch, P., Li, N., Milstein, S., Fan, C., Hao, T., Szabo, G., Hu, Z., Venkatesan, K., Bethel, G., Martin, P. *et al.* (2007) hORFeome v3.1: a resource of human open reading frames representing over 10,000 human genes. *Genomics*, **89**, 307-315.

76 Wang, X.J., Cao, Q., Liu, X., Wang, K.T., Mi, W., Zhang, Y., Li, L.F., LeBlanc, A.C. and Su, X.D. Crystal structures of human caspase 6 reveal a new mechanism for intramolecular cleavage self-activation. *EMBO Rep.*, **11**, 841-847.

77 Thomas, P.D., Campbell, M.J., Kejariwal, A., Mi, H., Karlak, B., Daverman, R., Diemer, K., Muruganujan, A. and Narechania, A. (2003) PANTHER: a library of protein families and subfamilies indexed by function. *Genome research*, **13**, 2129-2141.

78 Verspurten, J., Gevaert, K., Declercq, W. and Vandenabeele, P. (2009) SitePredicting the cleavage of proteinase substrates. *Trends Biochem Sci*, **34**, 319-323.

79 Hamosh, A., Scott, A.F., Amberger, J.S., Bocchini, C.A. and McKusick, V.A. (2005) Online Mendelian Inheritance in Man (OMIM), a knowledgebase of human genes and genetic disorders. *Nucleic acids research*, **33**, D514-517.

80 Barrios-Rodiles, M., Brown, K.R., Ozdamar, B., Bose, R., Liu, Z., Donovan, R.S., Shinjo, F., Liu, Y., Dembowy, J., Taylor, I.W. *et al.* (2005) High-throughput mapping of a dynamic signaling network in mammalian cells. *Science*, **307**, 1621-1625.

81 Braun, P., Tasan, M., Dreze, M., Barrios-Rodiles, M., Lemmens, I., Yu, H., Sahalie, J.M., Murray, R.R., Roncari, L., de Smet, A.S. *et al.* (2009) An experimentally derived confidence score for binary protein-protein interactions. *Nature methods*, **6**, 91-97.

82 Hermel, E., Gafni, J., Propp, S.S., Leavitt, B.R., Wellington, C.L., Young, J.E., Hackam, A.S., Logvinova, A.V., Peel, A.L., Chen, S.F. *et al.* (2004) Specific caspase interactions and amplification are involved in selective neuronal vulnerability in Huntington's disease. *Cell. Death.Differ.*, **11**, 424-438.

83 Suter, B., Fontaine, J.F., Yildirimman, R., Rasko, T., Schaefer, M.H., Rasche, A., Porras, P., Vazquez-Alvarez, B.M., Russ, J., Rau, K. *et al.* (2013) Development and application of a DNA microarray-based yeast two-hybrid system. *Nucleic acids research*, **41**, 1496-1507.

84 Hodges, A., Strand, A.D., Aragaki, A.K., Kuhn, A., Sengstag, T., Hughes, G., Elliston, L.A., Hartog, C., Goldstein, D.R., Thu, D. *et al.* (2006) Regional and cellular gene expression changes in human Huntington's disease brain. *Hum.Mol.Genet.*, **15**, 965-977.

85 Kuhn, A., Thu, D., Waldvogel, H.J., Faull, R.L. and Luthi-Carter, R. (2011) Population-specific expression analysis (PSEA) reveals molecular changes in diseased brain. *Nature methods*, **8**, 945-947.

86 Stroedicke, M., Bounab, Y., Strempel, N., Klockmeier, K., Yigit, S., Friedrich, R.P., Chaurasia, G., Li, S., Hesse, F., Riechers, S.P. *et al.* (2015) Systematic interaction network filtering identifies CRMP1 as a novel suppressor of huntingtin misfolding and neurotoxicity. *Genome research*, **25**, 701-713.

87 Liu, Y., Conaway, L., Rutherford Bethard, J., Al-Ayoubi, A.M., Thompson Bradley, A., Zheng, H., Weed, S.A. and Eblen, S.T. (2013) Phosphorylation of the alternative mRNA splicing factor 45 (SPF45) by Clk1 regulates its splice site utilization, cell migration and invasion. *Nucleic acids research*, **41**, 4949-4962.

88 Lee, K.K., Murakawa, M., Nishida, E., Tsubuki, S., Kawashima, S., Sakamaki, K. and Yonehara, S. (1998) Proteolytic activation of MST/Krs, STE20-related protein kinase, by caspase during apoptosis. *Oncogene*, **16**, 3029-3037.

89 Deng, Y., Pang, A. and Wang, J.H. (2003) Regulation of mammalian STE20-like kinase 2 (MST2) by protein phosphorylation/dephosphorylation and proteolysis. *J. Biol. Chem.*, **278**, 11760-11767.

90 Lee, K.K., Ohyama, T., Yajima, N., Tsubuki, S. and Yonehara, S. (2001) MST, a physiological caspase substrate, highly sensitizes apoptosis both upstream and downstream of caspase activation. *J. Biol. Chem.*, **276**, 19276-19285.

91 Kim, D., Shu, S., Coppola, M.D., Kaneko, S., Yuan, Z.Q. and Cheng, J.Q. (2010) Regulation of proapoptotic mammalian ste20-like kinase MST2 by the IGF1-Akt pathway. *PLoS One*, **5**, e9616.

92 Bowles, K.R. and Jones, L. (2014) Kinase signalling in Huntington's disease. *Journal of Huntington's disease*, **3**, 89-123.

93 Ooi, J., Hayden, M.R. and Pouladi, M.A. (2014) Inhibition of Excessive Monoamine Oxidase A/B Activity Protects Against Stress-induced Neuronal Death in Huntington Disease. *Molecular neurobiology*, in press.

94 Janicke, R.U., Sprengart, M.L., Wati, M.R. and Porter, A.G. (1998) Caspase-3 is required for DNA fragmentation and morphological changes associated with apoptosis. *J. Biol. Chem.*, **273**, 9357-9360.

95 Pompl, P.N., Yemul, S., Xiang, Z., Ho, L., Haroutunian, V., Purohit, D., Mohs, R. and Pasinetti, G.M. (2003) Caspase gene expression in the brain as a function of the clinical progression of Alzheimer disease. *Arch.Neurol.*, **60**, 369-376.

96 Gervais, F.G., Xu, D., Robertson, G.S., Vaillancourt, J.P., Zhu, Y., Huang, J., LeBlanc, A., Smith, D., Rigby, M., Shearman, M.S. *et al.* (1999) Involvement of caspases in proteolytic cleavage of Alzheimer's amyloid-beta precursor protein and amyloidogenic A beta peptide formation. *Cell*, **97**, 395-406.

97 Lu, D.C., Rabizadeh, S., Chandra, S., Shayya, R.F., Ellerby, L.M., Ye, X., Salvesen, G.S., Koo, E.H. and Bredesen, D.E. (2000) A second cytotoxic proteolytic peptide derived from amyloid beta-protein precursor. *Nat.Med.*, **6**, 397-404.

98 Klaiman, G., Petzke, T.L., Hammond, J. and LeBlanc, A.C. (2008) Targets of caspase-6 activity in human neurons and Alzheimer disease. *Mol.Cell Proteomics.*, **7**, 1541-1555.

99 Ju, W., Valencia, C.A., Pang, H., Ke, Y., Gao, W., Dong, B. and Liu, R. (2007) Proteome-wide identification of family member-specific natural substrate repertoire of caspases. *Proc. Natl. Acad. Sci. U S A*, **104**, 14294-14299.

100 Jung, J.Y., Lee, S.R., Kim, S., Chi, S.W., Bae, K.H., Park, B.C., Kim, J.H. and Park, S.G. (2014) Identification of novel binding partners for caspase-6 using a proteomic approach. *Journal of microbiology and biotechnology*, **24**, 714-718.

101 Ghavidel, A., Cagney, G. and Emili, A. (2005) A skeleton of the human protein interactome. *Cell*, **122**, 830-832.

102 von Mering, C., Krause, R., Snel, B., Cornell, M., Oliver, S.G., Fields, S. and Bork, P. (2002) Comparative assessment of large-scale data sets of protein-protein interactions. *Nature*, **417**, 399-403.

103 Waldron-Roby, E., Ratovitski, T., Wang, X., Jiang, M., Watkin, E., Arbez, N., Graham, R.K., Hayden, M.R., Hou, Z., Mori, S. *et al.* (2012) Transgenic Mouse Model Expressing the Caspase 6 Fragment of Mutant Huntingtin. *J. Neurosci.*, **32**, 183-193.

104 Zhao, M., Su, J., Head, E. and Cotman, C.W. (2003) Accumulation of caspase cleaved amyloid precursor protein represents an early neurodegenerative event in aging and in Alzheimer's disease. *Neurobiol.Dis.*, **14**, 391-403.

105 Guo, H., Albrecht, S., Bourdeau, M., Petzke, T., Bergeron, C. and LeBlanc, A.C. (2004) Active caspase-6 and caspase-6-cleaved tau in neuropil threads, neuritic plaques, and neurofibrillary tangles of Alzheimer's disease. *Am.J Pathol.*, **165**, 523-531.

106 Rohn, T.T., Head, E., Nesse, W.H., Cotman, C.W. and Cribbs, D.H. (2001) Activation of caspase-8 in the Alzheimer's disease brain. *Neurobiol. Dis.*, **8**, 1006-1016.

107 Ramcharitar, J., Albrecht, S., Afonso, V.M., Kaushal, V., Bennett, D.A. and Leblanc, A.C. (2013) Cerebrospinal Fluid Tau Cleaved by Caspase-6 Reflects Brain Levels and Cognition in Aging and Alzheimer Disease. *Journal of neuropathology and experimental neurology*, **72**, 824-832.

108 Harris, J.A., Devidze, N., Halabisky, B., Lo, I., Thwin, M.T., Yu, G.Q., Bredesen, D.E., Masliah, E. and Mucke, L. (2010) Many neuronal and behavioral impairments in transgenic mouse models of Alzheimer's disease are independent of caspase cleavage of the amyloid precursor protein. *J. Neurosci.*, **30**, 372-381.

109 Zhang, Y., Leavitt, B.R., Van Raamsdonk, J.M., Dragatsis, I., Goldowitz, D., Macdonald, M.E., Hayden, M.R. and Friedlander, R.M. (2006) Huntingtin inhibits caspase-3 activation. *The EMBO journal*, **25**, 5896-5906.

110 Rigamonti, D., Sipione, S., Goffredo, D., Zuccato, C., Fossale, E. and Cattaneo, E. (2001) Huntingtin's neuroprotective activity occurs via inhibition of procaspase-9 processing. *J. Biol.Chem.*, **276**, 14545-14548.

111 La Spada, A.R. and Morrison, R.S. (2005) The power of the dark side: Huntington's disease protein and p53 form a deadly alliance. *Neuron*, **47**, 1-3.

112 Tourette, C., Li, B., Bell, R., O'Hare, S., Kaltenbach, L.S., Mooney, S.D. and Hughes, R.E. (2014) A large scale Huntingtin protein interaction network implicates Rho GTPase signaling pathways in Huntington disease. *J Biol. Chem.*, **289**, 6709-6726.

113 Xifro, X., Anglada-Huguet, M., Rue, L., Saavedra, A., Perez-Navarro, E. and Alberch, J. (2011) Increased 90-kDa ribosomal S6 kinase (Rsk) activity is protective against mutant huntingtin toxicity. *Molecular neurodegeneration*, **6**, 74.

114 Plotkin, J.L., Day, M., Peterson, J.D., Xie, Z., Kress, G.J., Rafalovich, I., Kondapalli, J., Gertler, T.S., Flajolet, M., Greengard, P. *et al.* (2014) Impaired TrkB receptor signaling underlies corticostriatal dysfunction in Huntington's disease. *Neuron*, **83**, 178-188.

115 Gines, S., Ivanova, E., Seong, I.S., Saura, C.A. and MacDonald, M.E. (2003) Enhanced Akt signaling is an early pro-survival response that reflects N-methyl-D-aspartate receptor activation in Huntington's disease knock-in striatal cells. *J. Biol. Chem.*, **278**, 50514-50522.

116 Ehrnhoefer, D.E., Skotte, N.H., Ladha, S., Nguyen, Y.T., Qiu, X., Deng, Y., Huynh, K.T., Engemann, S., Nielsen, S.M., Becanovic, K. *et al.* (2014) p53 increases caspase-6 expression and activation in muscle tissue expressing mutant huntingtin. *Hum. Mol. Genet.*, **23**, 717-729.

117 MacLachlan, T.K. and el Deiry, W.S. (2002) Apoptotic threshold is lowered by p53 transactivation of caspase-6. *Proc.Natl.Acad.Sci.U.S.A*, **99**, 9492-9497.

118 Checler, F. and Alves da Costa, C. (2014) p53 in neurodegenerative diseases and brain cancers. *Pharmacology & therapeutics*, **142**, 99-113.

119 Rosner, M., Hanneder, M., Siegel, N., Valli, A., Fuchs, C. and Hengstschlager, M. (2008) The mTOR pathway and its role in human genetic diseases. *Mutation research*, **659**, 284-292.

120 Niu, Y.L., Li, C. and Zhang, G.Y. (2011) Blocking Daxx trafficking attenuates neuronal cell death following ischemia/reperfusion in rat hippocampus CA1 region. *Archives of biochemistry and biophysics*, **515**, 89-98.

121 Song, J.J. and Lee, Y.J. (2004) Daxx deletion mutant (amino acids 501-625)-induced apoptosis occurs through the JNK/p38-Bax-dependent mitochondrial pathway. *Journal of cellular biochemistry*, **92**, 1257-1270.

122 Bojunga, J., Nowak, D., Mitrou, P.S., Hoelzer, D., Zeuzem, S. and Chow, K.U. (2004) Antioxidative treatment prevents activation of death-receptor- and mitochondrion-dependent apoptosis in the hearts of diabetic rats. *Diabetologia*, **47**, 2072-2080.

123 Roubille, F., Combes, S., Leal-Sanchez, J., Barrere, C., Cransac, F., Sportouch-Dukhan, C., Gahide, G., Serre, I., Kupfer, E., Richard, S. *et al.* (2007) Myocardial expression of a dominant-negative form of Daxx decreases infarct size and attenuates apoptosis in an in vivo mouse model of ischemia/reperfusion injury. *Circulation*, **116**, 2709-2717.

124 Lukiw, W.J. (2004) Gene expression profiling in fetal, aged, and Alzheimer hippocampus: a continuum of stress-related signaling. *Neurochemical research*, **29**, 1287-1297.

125 Colangelo, V., Schurr, J., Ball, M.J., Pelaez, R.P., Bazan, N.G. and Lukiw, W.J. (2002) Gene expression profiling of 12633 genes in Alzheimer hippocampal CA1: transcription and neurotrophic factor down-regulation and up-regulation of apoptotic and pro-inflammatory signaling. *J. Neurosci. Res.*, **70**, 462-473.

126 Akterin, S., Cowburn, R.F., Miranda-Vizuete, A., Jimenez, A., Bogdanovic, N., Winblad, B. and Cedazo-Minguez, A. (2006) Involvement of glutaredoxin-1 and thioredoxin-1 in beta-amyloid toxicity and Alzheimer's disease. *Cell death and differentiation*, **13**, 1454-1465.

127 Corsini, L., Bonnal, S., Basquin, J., Hothorn, M., Scheffzek, K., Valcarcel, J. and Sattler, M. (2007) U2AF-homology motif interactions are required for alternative splicing regulation by SPF45. *Nature structural & molecular biology*, **14**, 620-629.

128 Akhavantabasi, S., Akman, H.B., Sapmaz, A., Keller, J., Petty, E.M. and Erson, A.E. (2010) USP32 is an active, membrane-bound ubiquitin protease overexpressed in breast cancers. *Mammalian genome : official journal of the International Mammalian Genome Society*, **21**, 388-397.

129 Graves, J.D., Draves, K.E., Gotoh, Y., Krebs, E.G. and Clark, E.A. (2001) Both phosphorylation and caspase-mediated cleavage contribute to regulation of the Ste20-like protein kinase Mst1 during CD95/Fas-induced apoptosis. *J Biol Chem*, **276**, 14909-14915.

130 Graves, J.D., Gotoh, Y., Draves, K.E., Ambrose, D., Han, D.K., Wright, M., Chernoff, J., Clark, E.A. and Krebs, E.G. (1998) Caspase-mediated activation and induction of apoptosis by the mammalian Ste20-like kinase Mst1. *The EMBO journal*, **17**, 2224-2234.

131 Lee, K.K. and Yonehara, S. (2002) Phosphorylation and dimerization regulate nucleocytoplasmic shuttling of mammalian STE20-like kinase (MST). *J Biol. Chem.*, **277**, 12351-12358.

132 van Raam, B.J., Ehrnhoefer, D.E., Hayden, M.R. and Salvesen, G.S. (2013) Intrinsic cleavage of receptor-interacting protein kinase-1 by caspase-6. *Cell death and differentiation*, **20**, 86-96.

133 Suzuki, A., Kusakai, G., Kishimoto, A., Shimojo, Y., Miyamoto, S., Ogura, T., Ochiai, A. and Esumi, H. (2004) Regulation of caspase-6 and FLIP by the AMPK family member ARK5. *Oncogene*, **23**, 7067-7075.

134 Kurokawa, M. and Kornbluth, S. (2009) Caspases and kinases in a death grip. *Cell*, **138**, 838-854.

135 Medina, E.A., Afsari, R.R., Ravid, T., Castillo, S.S., Erickson, K.L. and Goldkorn, T. (2005) Tumor necrosis factor-{alpha} decreases Akt protein levels in 3T3-L1 adipocytes via the caspase-dependent ubiquitination of Akt. *Endocrinology*, **146**, 2726-2735.

136 Warby, S.C., Chan, E.Y., Metzler, M., Gan, L., Singaraja, R.R., Crocker, S.F., Robertson, H.A. and Hayden, M.R. (2005) Huntingtin phosphorylation on serine 421 is significantly reduced in the striatum and by polyglutamine expansion in vivo. *Hum.Mol.Genet.*, **14**, 1569-1577.

137 Lee, H.K., Kumar, P., Fu, Q., Rosen, K.M. and Querfurth, H.W. (2009) The insulin/Akt signaling pathway is targeted by intracellular beta-amyloid. *Molecular biology of the cell*, **20**, 1533-1544.

138 Pouladi, M.A., Xie, Y., Skotte, N.H., Ehrnhoefer, D.E., Graham, R.K., Kim, J.E., Bissada, N., Yang, X.W., Paganetti, P., Friedlander, R.M. *et al.* (2010) Full-length huntingtin levels modulate body weight by influencing insulin-like growth factor 1 expression. *Hum Mol Genet*, **19**, 1528-1538.

139 Stelzl, U., Worm, U., Lalowski, M., Haenig, C., Brembeck, F.H., Goehler, H., Stroedicke, M., Zenkner, M., Schoenherr, A., Koeppen, S. *et al.* (2005) A human protein-protein interaction network: a resource for annotating the proteome. *Cell*, **122**, 957-968.

140 Palidwor, G.A., Shcherbinin, S., Huska, M.R., Rasko, T., Stelzl, U., Arumughan, A., Foulle, R., Porras, P., Sanchez-Pulido, L., Wanker, E.E. *et al.* (2009) Detection of alpha-rod protein repeats using a neural network and application to huntingtin. *PLoS Comput Biol*, **5**, e1000304.

141 Goehler, H., Lalowski, M., Stelzl, U., Waelter, S., Stroedicke, M., Worm, U., Droege, A., Lindenberg, K.S., Knoblich, M., Haenig, C. *et al.* (2004) A protein interaction network links GIT1, an enhancer of huntingtin aggregation, to Huntington's disease. *Mol. Cell.*, **15**, 853-865.

142 Kaltenbach, L.S., Romero, E., Becklin, R.R., Chettier, R., Bell, R., Phansalkar, A., Strand, A., Torcassi, C., Savage, J., Hurlburt, A. *et al.* (2007) Huntingtin interacting proteins are genetic modifiers of neurodegeneration. *PLoS Genet*, **3**, e82.

143 Schaefer, M.H., Fontaine, J.F., Vinayagam, A., Porras, P., Wanker, E.E. and Andrade-Navarro, M.A. (2012) HIPPIE: Integrating protein interaction networks with experiment based quality scores. *PLoS One*, **7**, e31826.

144 Jain, N., Thatte, J., Braciale, T., Ley, K., O'Connell, M. and Lee, J.K. (2003) Local-pooled-error test for identifying differentially expressed genes with a small number of replicated microarrays. *Bioinformatics*, **19**, 1945-1951.

145 Su, A.I., Wiltshire, T., Batalov, S., Lapp, H., Ching, K.A., Block, D., Zhang, J., Soden, R., Hayakawa, M., Kreiman, G. *et al.* (2004) A gene atlas of the mouse and human protein-encoding transcriptomes. *Proc Natl Acad Sci U S A*, **101**, 6062-6067.

146 Zhang, Y., Chen, K., Sloan, S.A., Bennett, M.L., Scholze, A.R., O'Keeffe, S., Phatnani, H.P., Guarnieri, P., Caneda, C., Ruderisch, N. *et al.* (2014) An RNA-sequencing transcriptome and splicing database of glia, neurons, and vascular cells of the cerebral cortex. *J Neurosci*, **34**, 11929-11947.

Legends for figures

Fig.1 Results of Y2H screen with caspase-6. A) Pro-CASP6 exists as a dimer with a 23aa prodomain and 14aa linker region between the large (p20) and small (p10) subunits. During activation each CASP6 monomer is cleaved at 3 sites thereby removing the prodomain and linker region. B) The initial screen, including CASP6 baits p34 (proform), p20 (active form) and p10 (active form), was against a 16,945 human cDNA library. The secondary de-convolution screen included 1,066 cDNAs. Top hits (87 interactors) were observed in triplicate on SD4 screen and triplicate or duplicate on LacZ screen. C) Network view of protein-protein interactions amongst CASP6 pro and active forms. The highest number of common interactions between CASP6 pro and active forms was observed between p34, p20 and p10 (34%). A large number of common interactions was also observed between p20 and p10 (28%).

Fig.2 Confirmation of select caspase-6 Y2H identified interactors by LUMIER. Proteins identified in the CASP6 Y2H screen that did not contain a "predicted" CASP6 recognition site were further validated using LUMIER. Six "predicted" CASP6 substrates were also included to provide additional validation of an interaction with CASP6. A total of 34 proteins were screened using LUMIER and 51% of the Y2H identified interactions confirmed.

Fig.3 Several caspase-6 interacting proteins are dysregulated in HD brain. A) Murine cortex lysates were subject to digestion with increasing concentrations of recombinant CASP6 for one hour or fixed concentration of CASP6 (15μM) and varying times of incubation. Western blotting demonstrates that CASP6 cleaves huntingtin using MAB2166 and B) BKP1 HTT antibodies. C) Network analysis demonstrates that a number of Y2H identified CASP6 interactors are involved in the pathogenesis of HD. Of the 87 interactors, 47 (54%) are dysregulated in human HD brain at the mRNA level and 9 are HTT interactors.

Fig. 4 Criteria for selecting potential caspase-6 substrates that may play a role in the pathogenesis of HD. In order to prioritize characterization, and maximize the opportunity of identifying novel CASP6 substrates involved in the pathogenesis of HD, Y2H identified proteins were assessed using the following criteria 1) high likelihood of cleavage by SitePrediction (99.9% specificity), 2) expressed in brain, 3) implicated in HD, 4) demonstrate an interaction with both p20 *and* p10 CASP6 baits, and 5) the biological function of the protein [implicated in excitotoxicity/signal transduction and/or apoptosis pathways]. The resultant proteins were then assessed in CASP6 cleavage assays.

Fig.5 Novel CASP6 substrates STK3 and DAXX identified. Murine cortex lysates were subject to digestion with increasing concentrations of recombinant CASP6 for one hour or fixed concentration of CASP6 (15μM) and varying times of incubation. Western blotting demonstrates that CASP6 cleaves A) death domain associated protein (DAXX). B) Diagram of DAXX protein showing structural (coiled coil) and nuclear localization signal (NLS) motifs. CASP6 also cleaves C) serine threonine kinase (STK3). D) Diagram of STK3 protein showing structural (coiled coil), kinase domain and adenosine 5' -triphosphate (ATP) motifs. Major cleavage fragments are highlighted by arrows. FL=full length form of protein. 'Predicted' CASP6 recognition sites are shown in blue.

Fig.6 Alterations in expression levels and post-translational modifications of STK3 observed in acute and chronic models of HD. A) Immortalized striatal cells with ($STHdh^{Q111}$) and without ($STHdh^{Q7}$) mutant HTT were incubated ± serum and using Western blotting assessed at 24hrs post starvation for protein expression of STK3 (n=3). Controls include $STHdh^{Q7}$ lysate ±CASP6. B) A significant increase in full length (FL) levels of the pro-apototic kinase, STK3, is observed in striatal cells expressing mutant HTT compared to WT at baseline (ANOVA $p<0.017$, post hoc $STHdh^{Q7}(+)$ vs. $STHdh^{Q111}(+)$ $p<0.05$). In contrast, FL levels of STK3 are decreased in $STHdh^{Q111}(-)$ compared to $STHdh^{Q111}(+)$ cells (post hoc $p<0.05$) as expected due to the cleavage of STK3. C) A significant increase in fragment levels of STK3 is observed in cells expressing

mutant HTT compared to WT post serum starvation (ANOVA $p<0.0001$, post hoc $STHdh^{Q7}$(-) vs. $STHdh^{Q111}$(-) $p<0.001$). D) Evaluation of cell death in serum starved $STHdh^{Q7}$ and $STHdh^{Q111}$ cells demonstrates that a significant increase in cell death is observed in $STHdh^{Q111}$ cells 12 and 24hrs post starvation. Tubulin was used as a loading control.

Fig.7 Cleavage of STK3 in the absence of caspase-3. Alterations in expression levels and post-translational modifications of STK3 are observed in stressed MCF7 cells. A) Incubation of murine cortex with either recombinant casp3 or CASP6 demonstrates that both caspase-3 and caspase-6 cleave STK3. However, caspase-3 generates a single cleavage fragment while in contrast caspase-6 generates 3 cleavage fragments of STK3. In addition, B) Western blotting demonstrates that MCF7 cells, which lack caspase-3, stressed with campothecin show a decrease in full-length STK3 levels and an increase in STK3 fragments compared to unstressed MCF7 cells. C) A significant decrease in full-length (FL) levels of STK3 is observed in in MCF7 cells post camptothecin stress ($n=4$, $p<0.001$). D) Furthermore, a significant increase in STK3 fragment levels is observed in MCF7 cells post stress ($n=4$, $p<0.001$). In contrast, the STK3 fragment was not detected in stressed MCF7 cells pretreated with the pan caspase inhibitor Q-VD-OPh. Actin was used as a loading control.

Tables

Table.1 Top CASP6 Y2H identified potential CASP6 substrates that may play a role in the pathogenesis of HD.

Gene Symbol	Dysregulated in human HD brain	Excitotoxocity/Signal transduction	Apoptosis
BAIAP2	↓[a] ↓[b]		
GSK3A	↓[a]		
STX16	↑[a] ↑[b] ↑[c]		
PALMD	↑[a]		
P13KR1	↑[a] ↑[b]		
DAXX	↑[a]		
STK3	↑[a] ↑[b]		
USP32	↓[a]		
RBM17	↑[a] ↑[b]		

[a]In grade 1-4 human HD brain vs. control

[b]In grade 1 human HD brain vs. control

[c]In HD astrocytes vs. control

Table.2 Summary of CASP6 Y2H identified interactors assessed in CASP6 cleavage assays.

Gene Symbol	Predicted CASP6 sites [SitePrediction]	Validated [cleavage assay]	# cleavage fragments
DAXX	15	YES	7
PALMD	7	YES	4
USP32	5	YES	3
PIK3R1	5	NO	0
RBM17	5	YES	1
STK3	3	YES	2
BAIAP2	2	NO	0
STX16	2	YES	1
GSK3A	1	NO	0

Table.3 Result of Panther analysis on validated CASP6 interactors

Pathway	p value	Fold Enrichment
FAS signaling	p=7.05E-10	>5
HD	p=1.94E-08	>5
Apoptosis signaling	p=3.84E-06	>5
Gonadotropin releasing hormone receptor	p=0.002	>5
AD-presenilin	p=0.004	>5
Molecular function	**p value**	
Structural constituents - cytoskeleton	p=1.93E-11	4.9
Structural molecule activity	p=5.98E-09	3.6
Protein binding	p=2.03E-06	2.3
Cysteine-type peptidase activity	p=0.0003	>5
Cytoskeletal protein binding	p=0.004	>5

Peptidase Inhibitor activity	**p=0.003**	**>5**
Protein class	**p value**	
Cytoskeletal	**p=9.36E-14**	**>5**
Anatomical structural	**p=1.79E-10**	**>5**
Metabolic process	**p=3.14E-07**	**1.6**
Intermediate filament	**p=5.74E-06**	**>5**
Actin cytoskeletal	**p=0.0005**	**4.4**
Proteolysis	**p=0.0004**	**3.2**

All values are post Bonferroni correction.

Abbreviations

APP – Amyloid beta precursor protein

BAIAP2 - Brain-specific angiogenesis inhibitor 1-associated protein 2

CASP6 – Caspase-6

CE – Cerebellum

CN – Caudate nucleus

DAXX - Death domain associated protein

GSK3A - Glycogen synthase kinase-3 alpha

HTT – huntingtin

INFIDEX (**i**nteraction **n**etwork **fi**ltering by **d**ifferentially **ex**pressed genes)

LDH – Lactate dehydrogenase

MC – Motor cortex

mHTT – mutant huntingtin

PALMD - Palmdelphin

PFC – Prefronal cortex

P13KR1 - Phosphoinositide-3-kinase, regulatory subunit 1 (alpha)

PPI – Protein-protein interaction

RBM17 - RNA binging motif 17

STK3 - serine threonine kinase

STX16 - Syntaxin 16

USP32 - Ubiquitin specific peptidase

Y2H – Yeast-two-hybrid

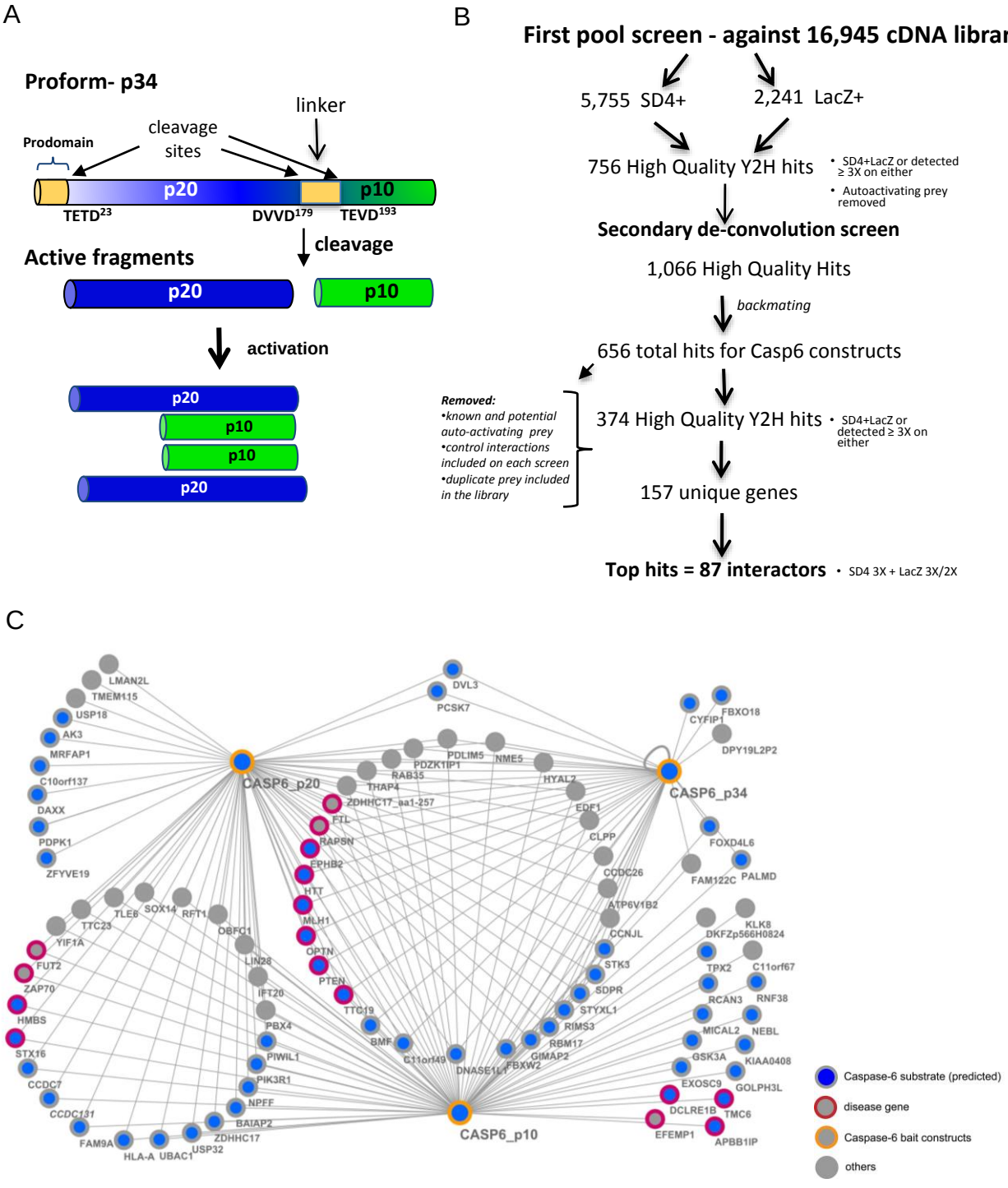
A
Proform- p34
linker
cleavage sites
Prodomain
p20
p10
TETD23
DVVD179
TEVD193
cleavage
Active fragments
p20
p10
activation
p20
p10
p10
p20
B
First pool screen - against 16,945 cDNA library
5,755 SD4+
2,241 LacZ+
756 High Quality Y2H hits
• SD4+LacZ or detected ≥ 3X on either
• Autoactivating prey removed
Secondary de-convolution screen
1,066 High Quality Hits
backmating
656 total hits for Casp6 constructs
Removed:
•known and potential auto-activating prey
•control interactions included on each screen
•duplicate prey included in the library
374 High Quality Y2H hits
• SD4+LacZ or detected ≥ 3X on either
157 unique genes
Top hits = 87 interactors
• SD4 3X + LacZ 3X/2X
C
CASP6_p20
CASP6_p34
CASP6_p10
Caspase-6 substrate (predicted)
disease gene
Caspase-6 bait constructs
others

Figure.1

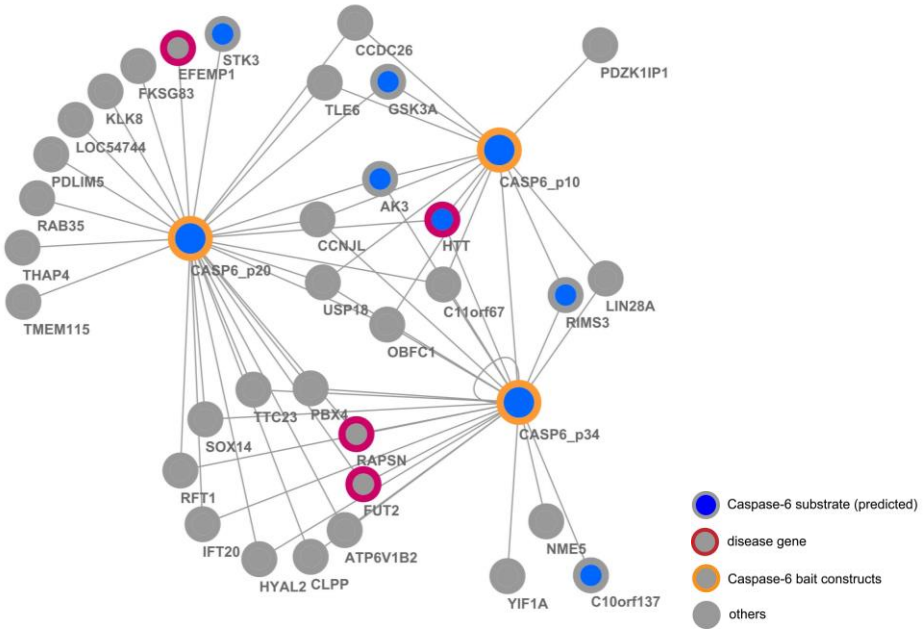
STK3
EFEMP1
FKSG83
KLK8
LOC54744
PDLIM5
RAB35
THAP4
TMEM115
CCDC26
TLE6
GSK3A
PDZK1IP1
CASP6_p10
AK3
HTT
CCNJL
CASP6_p20
USP18
C11orf67
OBFC1
LIN28A
RIMS3
TTC23
PBX4
SOX14
RAPSN
CASP6_p34
RFT1
FUT2
IFT20
ATP6V1B2
HYAL2
CLPP
NME5
YIF1A
C10orf137
Caspase-6 substrate (predicted)
disease gene
Caspase-6 bait constructs
others

Figure.2

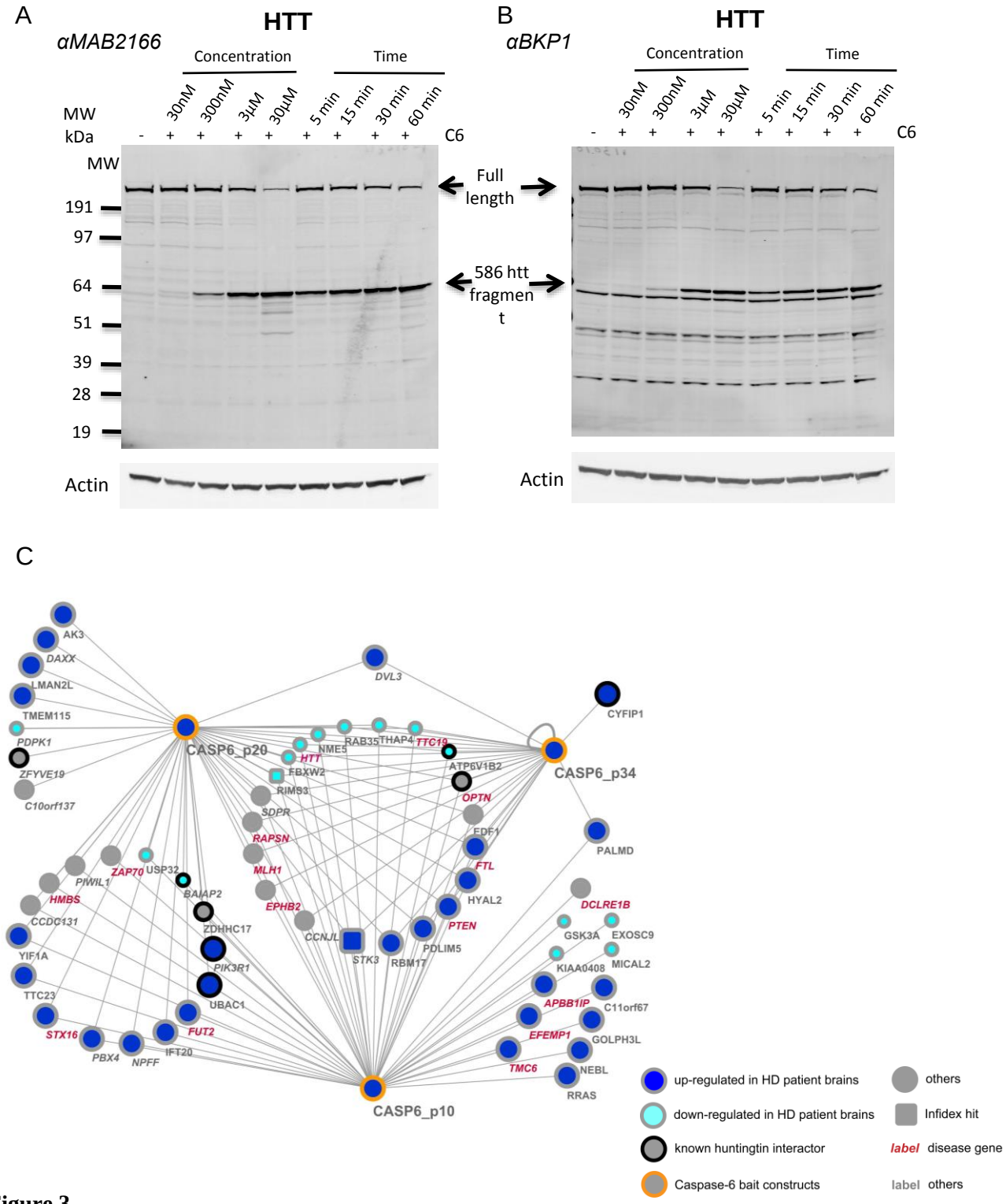
A
αMAB2166
HTT
Concentration
Time
30nM
300nM
3μM
30μM
5 min
15 min
30 min
60 min
MW
kDa
C6
MW
191
97
64
51
39
28
19
Full length
586 htt fragment
Actin
B
αBKP1
HTT
Concentration
Time
C6
Actin
C
AK3
DAXX
LMAN2L
TMEM115
PDPK1
ZFYVE19
C10orf137
DVL3
CASP6_p20
NME5
RAB35
THAP4
TTC19
HTT
FBXW2
RIMS3
SDPR
RAPSN
MLH1
EPHB2
CCNJL
STK3
RBM17
PDLIM5
PTEN
HYAL2
FTL
EDF1
OPTN
ATP6V1B2
CASP6_p34
CYFIP1
PALMD
DCLRE1B
GSK3A
EXOSC9
KIAA0408
MICAL2
APBB1IP
C11orf67
EFEMP1
GOLPH3L
TMC6
NEBL
RRAS
CASP6_p10
ZAP70
USP32
PIWIL1
BAIAP2
HMBS
CCDC131
ZDHHC17
YIF1A
PIK3R1
TTC23
UBAC1
STX16
PBX4
NPFF
IFT20
FUT2
up-regulated in HD patient brains
down-regulated in HD patient brains
known huntingtin interactor
Caspase-6 bait constructs
others
Infidex hit
label disease gene
label others

Figure.3

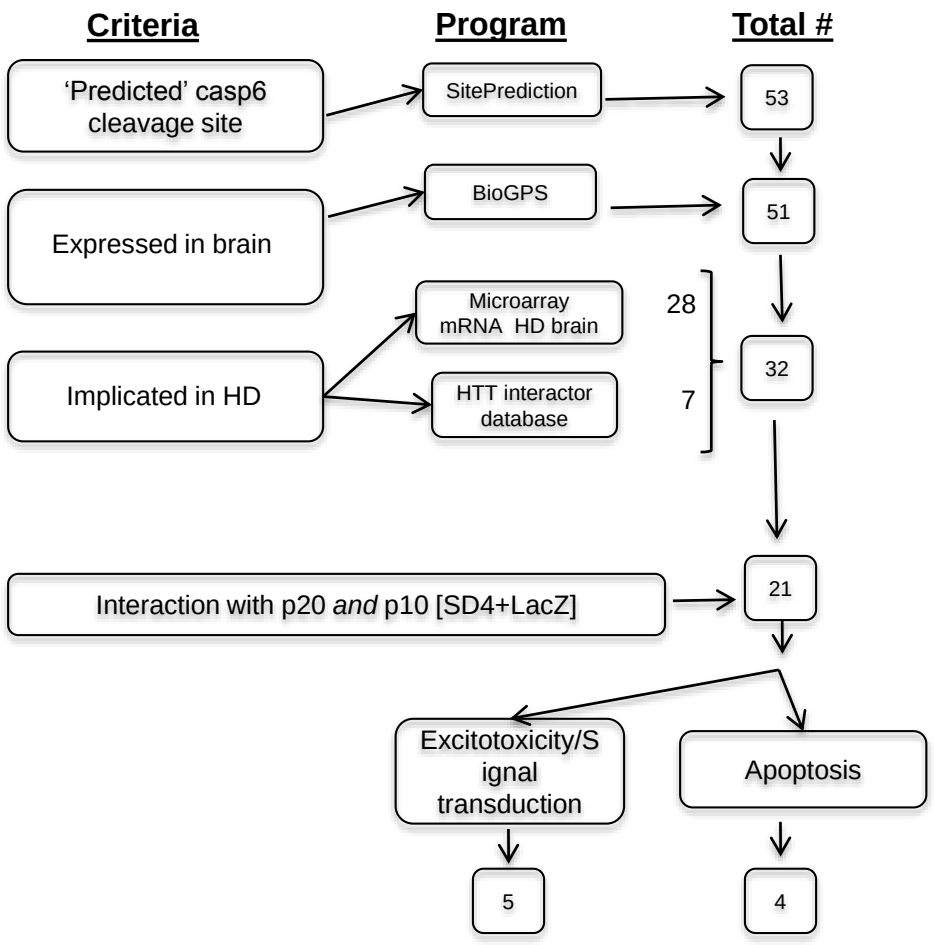
Prioritization criteria for assessment of potential substrates
Criteria
Program
Total #
'Predicted' casp6 cleavage site
SitePrediction
53
Expressed in brain
BioGPS
51
Implicated in HD
Microarray mRNA HD brain
HTT interactor database
28
7
32
Interaction with p20 and p10 [SD4+LacZ]
21
Excitotoxicity/Signal transduction
Apoptosis
5
4

Figure.4

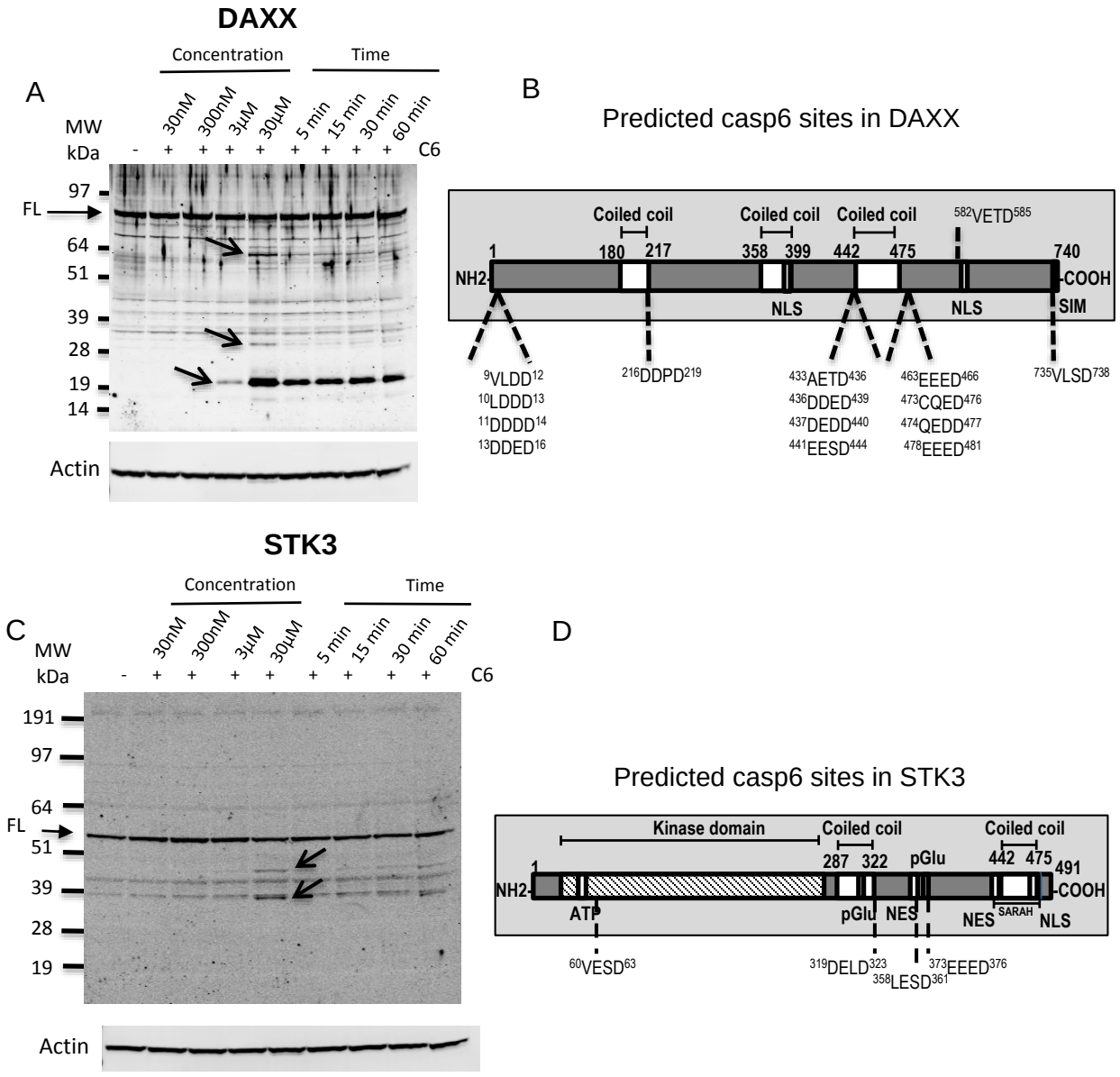
DAXX
Concentration
Time
A
MW
kDa
30nM
300nM
3µM
30µM
5 min
15 min
30 min
60 min
C6
97
64
51
39
28
19
14
FL
Actin
B
Predicted casp6 sites in DAXX
Coiled coil
Coiled coil
Coiled coil
582VETD585
1
180
217
358
399
442
475
740
NH2
COOH
NLS
NLS
SIM
9VLDD12
10LDDD13
11DDDD14
13DDED16
216DDPD219
433AETD436
436DDED439
437DEDD440
441EESD444
463EEED466
473CQED476
474QEDD477
478EEED481
735VLSD738
STK3
Concentration
Time
C
MW
kDa
30nM
300nM
3µM
30µM
5 min
15 min
30 min
60 min
C6
191
97
64
51
39
28
19
FL
Actin
D
Predicted casp6 sites in STK3
Kinase domain
Coiled coil
Coiled coil
1
287
322
pGlu
442
475
491
NH2
COOH
ATP
pGlu
NES
NES
SARAH
NLS
60VESD63
319DELD323
358LESD361
373EEED376

Figure.5

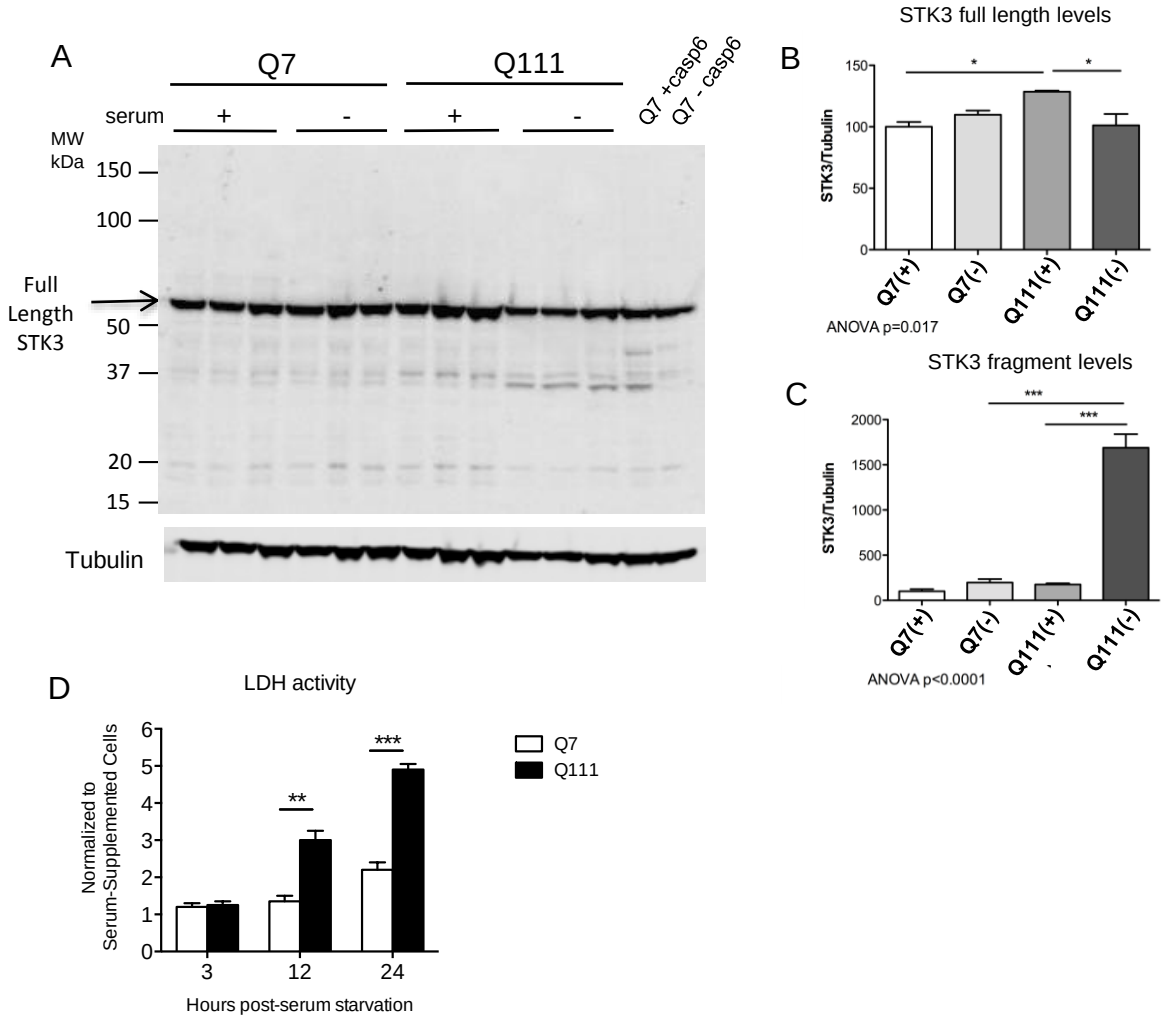
A
Q7
Q111
Q7 +casp6
Q7 - casp6
serum
+
-
+
-
MW
kDa
150
100
Full
Length
STK3
50
37
20
15
Tubulin
B
STK3 full length levels
STK3/Tubulin
150
100
50
0
*
*
Q7(+)
Q7(-)
Q111(+)
Q111(-)
ANOVA p=0.017
C
STK3 fragment levels
***
***
STK3/Tubulin
2000
1500
1000
500
0
Q7(+)
Q7(-)
Q111(+)
Q111(-)
ANOVA p<0.0001
D
LDH activity
Normalized to
Serum-Supplemented Cells
6
5
4
3
2
1
0
**
***
Q7
Q111
3
12
24
Hours post-serum starvation

Figure.6

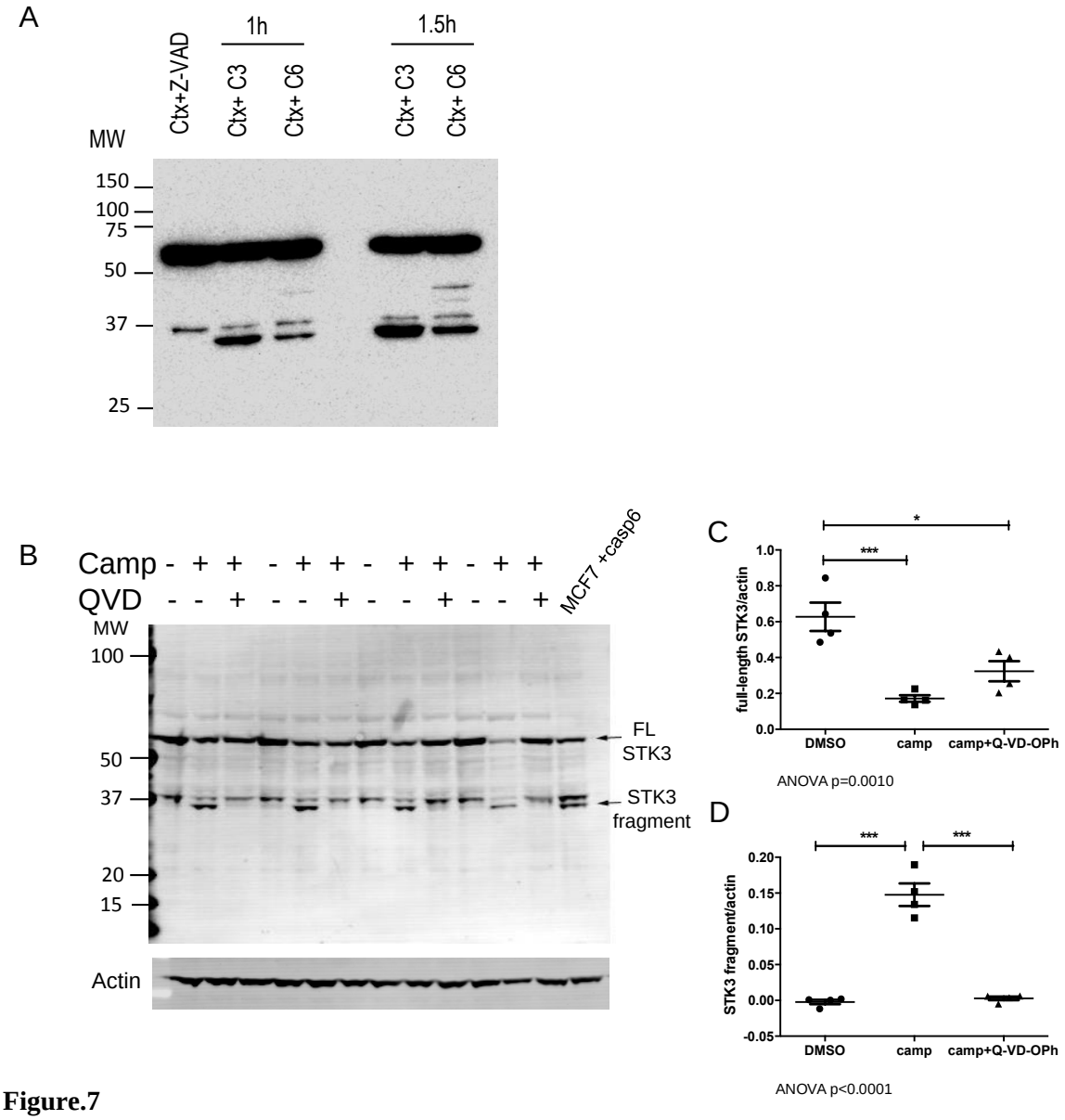
A
1h
1.5h
Ctx+Z-VAD
Ctx+ C3
Ctx+ C6
Ctx+ C3
Ctx+ C6
MW
150
100
75
50
37
25
B
Camp - + + - + + - + + - + +
QVD - - + - - + - - + - - +
MCF7 +casp6
MW
100
50
37
20
15
FL STK3
STK3 fragment
Actin
C
full-length STK3/actin
1.0
0.8
0.6
0.4
0.2
0.0
*
***
DMSO
camp
camp+Q-VD-OPh
ANOVA p=0.0010
D
STK3 fragment/actin
0.20
0.15
0.10
0.05
0.00
-0.05
***
***
DMSO
camp
camp+Q-VD-OPh
ANOVA p<0.0001

Figure.7